NASA TECHNICAL MEMORANDUM

NASA TM X-68031

NASA TM X-68031

OPTIMIZATION OF ENGINES FOR A COMMERCIAL MACH 0.93 TRANSPORT USING ADVANCED TURBINE COOLING METHODS

by Gerald A. Kraft, and John B. Whitlow, Jr.
Lewis Research Center
Cleveland, Ohio
March, 1972

This information is being published in preliminary form in order to expedite its early release.

ABSTRACT

A study was made of an advanced technology airplane using supercritical aerodynamics. Cruise Mach number was 0.98 at 40 000 feet altitude with a payload of 60 000 pounds and a range of 3000 nautical miles. Separate-flow turbofans were examined parametrically to determine the effect of sea-level-static design turbine-inlet-temperature ($T_{4\text{-sls}}$) and noise on takeoff gross weight (TOGW) assuming full-film turbine cooling. The optimum $T_{4\text{-sls}}$ was 2650° F. Two-stage-fan engines, with cruise fan pressure ratio (FPR_{cr}) of 2.25, achieved a noise goal of 103.5 EPNdB with todays noise technology while one-stage-fan engines, FPR_{cr} of 1.90, achieved a noise goal of 98 EPNdB. The TOGW penalty to use the one-stage fan was 6.2 percent.

E-6848

OPTIMIZATION OF ENGINES FOR A COMMERCIAL MACH 0.98 TRANSPORT USING ADVANCED TURBINE COOLING METHODS

by Gerald A. Kraft, and John B. Whitlow, Jr.

Lewis Research Center

E-6848

SUMMARY

A parametric study was made of a group of separate-flow-turbofan engines for use in advanced technology airplanes designed for a cruise speed of Mach 0.98 of 40 000 feet. The three-engined airplanes were sized to carry 300 passengers 3000 nautical miles. Cruise lift-drag ratios compatible with the supercritical wing were assumed. Fan and compressor pressure ratio, bypass ratio, and sea-level-static turbine-rotor-inlet-temperature ($T_{4\text{-sls}}$) were variables in the engine studied. $T_{4\text{-sls}}$ was varied from 2300° to 3000° F. The cruise T_4 was always 100° F less than the $T_{4\text{-sls}}$. Full coverage film cooling was used in the turbine. Engine weight varied with all major engine cycle parameters. Takeoff and climb constraints were observed. Combined jet and machinery noise levels (EPNdB) were calculated for selected engines at both the sideline (lift-off) and approach measuring stations specified in FAR Part 36.

It was found that a noise goal of 101 EPNdB (FAR-36 minus 5 EPNdB) could be met with two-stage fan engines having a cruise fan pressure ratio of 2.25. About 18 PNdB of fan machinery noise suppression was needed to achieve this goal. The minimum takeoff gross weight (TOGW) and direct operating cost (DOC) occurred at a $T_{4\text{-sls}}$ of 2650° F. With 20 PNdB of fan machinery noise suppression, one-stage fan engines having a cruise fan pressure ratio of 1.90 could meet a noise goal of 91 EPNdB (FAR-36 minus 15 EPNdB). At this fan pressure ratio, the minimum TOGW and DOC occurred at a $T_{4\text{-sls}}$ of 2650° F. Both the TOGW and the DOC increased about 8 percent for the best one-stage fan at the noise goal of 91 EPNdB compared to the best two-stage fan at a noise goal of 101 EPNdB.

INTRODUCTION

The supercritical wing proposed by Whitcomb (ref. 1) offers the potential for delaying the transonic drag rise experienced by present day subsonic jet transports as their flight speed approaches Mach 1.0. Transports using this wing could cruise at the same speed as today's transports with less drag or they could cruise at somewhat higher speeds with little or no penalty in lift-drag ratio (L/D).

Previous studies (refs. 2 and 3) have been made to define the optimum engine design parameters for a Mach 0.98 advanced technology transport. In reference 2 T_4 was allowed to vary assuming convection cooling for the turbine. In reference 3, very low noise goals were assumed to determine the need and direction for advanced noise suppression research. In reference 4, cruise Mach numbers from 0.90 to 0.98 were studied at one $T_{4\text{-sls}}$. The purpose of this study was to investigate the effect of high T_4 on the advanced technology transport with an advanced turbine cooling scheme (full-coverage film). Unlike reference 2, 3, or 4, the turbine cooling airflow was calculated in this study for each stator and rotor. The number of low pressure turbine stages was estimated for each engine so that consistant turbine cooling calculations could be made. The effects of varying T_4 are weighed in terms of TOGW and DOC at several noise goals as low as 91 EPNdB. The DOC was calculated by the ATA method of reference 5. The effect of advanced noise suppression techniques and reductions in machinery source noise are evaluated.

The range was fixed at 3000 nautical miles and the payload was held at 60 000 pounds (300 passengers). As engine design varied, the changes in engine weight, drag, and fuel requirements caused TOGW to vary. The T_4 at cruise was varied for each takeoff T_4 so as to minimize the TOGW. However cruise T_4 was never allowed to exceed takeoff T_4 minus 100° F. This restraint assured an adequate thrust margin for acceleration and climb up to cruise.

Climb and letdown fuel weights were considered to be a linear function of TOGW. A nominal value of cruise L/D was assumed as in references 2 and 3. As engine pod size changed from the reference size,

airplane cruise L/D was adjusted. It was assumed that wave drag changes could be largely eliminated by re-area-ruling the airplane as engine pods changed size.

As in reference 4, a component-matching computer program was used to correlate cruise, takeoff and approach engine parameters such as FPR, OPR, BPR, and W_a. The jet noise was calculated by the SAE standard method of references 7 and 8 (assuming two separate streams). The machinery noise was considered to be a function of FPR, the number of fan stages, distance and thrust. The two-stage fan was considered to be 6 PNdB louder than the one-stage fan at any given FPR. This is in contrast to references 2 to 4 where it was considered to be 8 PNdB louder. Jet and machinery noise were added to get the total noise at any point.

SYMBOLS

BPR	bypass ratio
Bleed	total cooling bleed for turbines, fraction of compressor exit air
C_{eng}	cost of each engine, dollars
C_L	lift coefficient
C_s	speed of sound (n mi/hr) knots
D	drag, lb
FA	fuel to air ratio
FN	net thrust, lb
FPR	fan pressure ratio
ΔH_{AB}	change in enthalpy between station A and B, Btu/lb
L	lift, lb
M	Mach number
OEW	operating empty weight, lb
OPR	overall fan and compressor pressure ratio

P	total pressure, lb/ft^2
R	range, n mi
S_{wing}	wing planform reference area, ft^2
SPL	sound pressure level, dB
sfc	specific fuel consumption (lb fuel/hr)/lb thrust
T	total temperature, ^oF
T_{ci}	initial cooling air total temperature, ^oF
T_{gi}	initial gas total temperature, ^oF
TOGW	takeoff gross weight, lb
$V_{fan-tip}$	sea-level-static fan tip speed, ft/sec
W_a	total airflow per engine, lb/sec
W_c	coolant flow, lb/sec
W_{end-cr}	airplane gross weight at the end of cruise, lb
W_{eng}	installed weight of three engines, lb
$W_{start-cr}$	airplane gross weight at start of cruise, lb
δ	pressure parameter, P/2116
θ	temperature parameter, (T + 460)/519
φ	turbine cooling parameter, $(T_{gi} - T_m)/(T_{gi} - T_{ci})$
Subscripts:	
cr	cruise
m	bulk metal temperature of blade, ^oR
sls	sea-level-static
1	fan face station
2	fan discharge station
3	inner compressor discharge station
4	turbine-rotor-inlet station

5 high pressure turbine exit station

6 low pressure turbine exit station

METHOD OF ANALYSIS

Selection of Reference TOGW and Airframe Weight

As in references 2 to 4, it was desired to select a reference airframe with which to match the various parametric engines. Range was initially calculated by the following equation.

$$R = 350 + \frac{(L/D)_{cr} M_{cr} C_s}{sfc} \ln \frac{W_{start-cr}}{W_{end-cr}}$$

The 350 term represents the climb range, 200 n mi, plus the letdown range, 150 n mi. The other terms on the right side of the equation represent the range for a Breguet cruise.

After an iteration described in references 2 to 4, the reference TOGW was selected as 386 000 pounds for a range of 3000 n mi. The reference airframe weight excluding engine was 180 000 pounds. After establishing the reference airplane, the range was fixed at 3000 n mi and the figure of merit in this report became TOGW. According to data from reference 6, airframe weight will remain nearly a constant fraction of TOGW over a considerable range of TOGW when the size of large transports is scaled up or down. However, if the fuselage is held constant (as it was in this study) the fraction will change slightly as shown in figure 1. The reason the fuselage was fixed was because the payload was fixed at 60 000 pounds (300 passengers at 200 pounds each). M_{cr} was selected as 0.98 and cruise was always started at 40 000 feet. Cruise L/D will be discussed later. Fuel for climb and letdown was calculated by the following equations.

$$\text{Fuel climb} = \frac{TOGW}{386\,000} \times 20\,000 \text{ pounds}$$

$$\text{Fuel letdown} = \frac{\text{TOGW}}{386\ 000} \times 2000 \text{ pounds}$$

The 386 000 pounds is the TOGW of the reference airplane and the 20 000 and 2000 pounds are the fuel assumed for climb and letdown of the reference airplane. The reserve fuel was always assumed to be 18 percent of the total fuel load.

A sketch of the study airplane is shown in figure 2. In the sketch, the engines are installed in the rear of the airplane. Other options such as having one in the tail and one under each wing may offer certain advantages. However, their location would have no impact on the way this study was done or its results. A sketch of a typical high BPR, separate-flow turbofan engine is shown in figure 3. Note the acoustic lining in the inlet and duct walls for the reduction of fan machinery noise. In addition, inlet and duct splitter rings are shown with sound deadening material. Different amounts of treatment are required to achieve different amounts of suppression. The weight and amount of these materials needed will be discussed later.

Lift-Drag Ratio

The L/D used for the reference airplane in this study was 16.8. This value was obtained through consideration of present day transports and test data for advanced transports as discussed in reference 4. This value of L/D includes the drag of three, 80-inch-diameter nacelles. The drag of one of the 80-inch engine nacelles is shown as a circled reference point on figure 4. The L/D ratio was adjusted by means of the curve shown in this figure as the engine nacelle diameter varied from 80 inches. The nacelle drag curve of figure 4 agrees with those in use by the engine and airframe manufacturers. By far the greatest part of this nacelle drag is due to friction. It is assumed that when nacelle size is changed, changes in wave drag can be area-ruled out by reconfiguring the fuselage as necessary. If the reference L/D was somewhat lower than 16.8, the airplane TOGW would be greater. However, L/D would have to be reduced by a large amount to have any effect on

the optimum cycle except for design W_a.

The only aerodynamic data available at the time of this study was the cruise L/D value discussed and an estimate of the approach L/D. The lack of climb aerodynamics is probably not too important to the calculations since only a small part of the mission was conducted at other than cruise conditions. The approach L/D was estimated to be about 5.5 at an approach speed of 135 knots. This value was needed to determine the approach thrust to be used in the noise calculations.

Engines

Cycle calculations were made for two-spool separate-flow turbofan engines in this study. Only two cruise fan pressure ratios were considered, 1.90 and 2.25. The FPR of 1.90 was chosen because it is approximately the maximum currently achievable with a single-stage fan with conventional blade loading. Single-stage fans are desirable because they are thought to produce less machinery noise with present technology than a two-stage fan at the same FPR (ref. 9). However, higher FPR's are desirable because they improve performance (refs. 2 and 3). Cruise FPR's higher than 2.25 were not considered because data presented in reference 3 indicated that more than 20 PNdB of fan machinery noise suppression may be needed to meet a 106 PNdB noise goal. As discussed in references 4 and 17, 15 PNdB suppression may be possible today and 20 PNdB of suppression may be available in a few years.

Cruise bypass ratios from 0.5 to 12 and overall pressure ratios from 20 to 52 were considered. The sea-level-static T_4 was varied from 2300° to 3000° F. The engines were sized such that the cruise T_4 was never higher than the takeoff T_4 minus 100° F. This 100° F insured reasonable thrust margin during climb and reasonable time up to cruise. The actual cruise T_4 could be determined only after several values of cruise T_4 had been tried to determine which one gave the minimum TOGW. In the case of this report, the optimum $T_{4\text{-cr}}$ was always 100° F less than $T_{4\text{-sls}}$.

In contrast to references 2, 3, or 4, no turbine cooling schedule was assumed in this report. Instead, an advanced cooling scheme - full coverage film - was assumed and the cooling for each stator and rotor was calculated at takeoff levels of T_4. In order to do this, the number of stages in the turbine had to be established. It was assumed that the high-pressure turbine consisted of one stator and one rotor. The cooling for the first stator was not calculated since our cycle calculations deal with T_4, the rotor-inlet temperature. Any stator cooling airflow is included in the combustor airflow and will not be included in any cooling bleed discussions or numbers from here on. It re-enters the main stream through the first stator and is mixed before station 4, the number of low-pressure turbine stages can be as few as one at low BPR's or as great as 10 or more at high BPR's. The following equation was derived to calculate the number of low-pressure turbine stages necessary for any engine

$$\text{Number of stages} = 9660 \frac{(1 + \text{BPR})(P_6/P_1)(\Delta H_{6,5})}{\left[1 + FA_4(1 - \text{Bleed})\right](V^2)_{\text{fan-tip}}\sqrt{T_6/T_1}}$$

Several assumptions are necessary before this equation can be derived. One of these is a schedule of corrected fan-tip speed versus FPR. The schedule used is shown in figure 5 for one-stage fans. For two-stage fans, the same curve was used but the square root of FPR was used to obtain $V_{\text{fan-tip}}$. The curve is a linear approximation tangent to the curve in reference 10 for a fan blade loading of 0.3 at a $V_{\text{fan-tip}}$ of 1900 ft/sec. (A complete explanation of the turbine cooling calculations, numbers of low pressure turbine stages calculations, and the assumptions are given in appendix A.)

This procedure for turbine design obviously is not exact, but it gave good results when tested against more elaborate ways of estimating the number of stages.

Knowing the number of stages and the delta H and delta T across each stage, the cooling bleed could be calculated for each stage. This was done with the aid of figure 6 which was obtained from reference 11. Figure 6 is based on laboratory tests of full-coverage film cooled vanes

tested in Allison's high temperature cascade rig. The blades were of advanced design using advanced fabrication techniques. φ was calculated for each stage as shown in appendix A. The bulk metal temperature of the blade (T_m) was fixed at 2110° R for the rotors and 2460° R for the stators. The initial total temperature of the cooling flow (T_{ci}) was set as the compressor exit temperature since the cooling bleed flow came from there. The actual gas total temperature initially passing the blade, T_{gi}, was obtained from cycle calculations. All of the bleeds were multiplied by a factor of 1.333 to account for wall and shroud cooling. The individual bleeds were added to give the total cooling bleed. If this was different than the assumed value of bleed, the new value was used and the cycle calculation was repeated as necessary. Thus, a consistant trend of cooling requirements at both high and low T_4's was obtained.

All the engines in this study were designed at cruise and operated off-design at takeoff. The correction factors that are applied to the design engine parameters to obtain their sea-level-static values were obtained by using a component-matching computer program (refs. 12 and 13). This program uses the actual component maps in the matching procedure. The correction factors (i.e., the sea-level-static value divided by the cruise value of the parameter) were plotted against BPR_{cr}. The factors plotted were corrected airflow at the fan face, fan pressure ratio, compressor pressure ratio, and bypass ratio. These factors were found to be relatively insensitive to overall pressure ratio within the limits listed except near the maximum BPR at which the engine would run. The correction factors that were used for a cruise FPR of 1.9 are shown in figure 7(a) to (d). A separate curve was plotted for each $T_{4\text{-sls}}$. Similar curves are shown in figure 8(a) to (d) for a cruise FPR of 2.25. During component-matching procedures at off-design, nozzle exhaust areas were maintained at their cruise values.

During approach the component-matching program was again used to find the part-power operating conditions needed. The approach conditions were assumed to be 370 feet altitude and 135 knots (Mach 0.203). The aircraft was assumed to have a 10° angle of attack, 3° glide slope, and an L/D of 5.5. Under these conditions the thrust was generally

about one-third of maximum.

At each cruise design point, the component efficiencies, pressure losses, coefficients, etc. were as follows:

Fan adiabatic efficiency	0.86
Compressor adiabatic efficiency	0.86
Combustor adiabatic efficiency	0.99
Inner turbine adiabatic efficiency	0.89
Outer turbine adiabatic efficiency	0.88
Inlet pressure recovery	0.98
Pressure ratio across combustor	0.96
Total duct pressure ratio from fan discharge to nozzle	0.94
Total core pressure ratio from low pressure turbine discharge to nozzle	0.98
Exhaust nozzle thrust coefficient (both streams)	0.98

Installed engine weight and dimensions were allowed to vary with changes in engine sea-level-static parameters as described by reference 14. This correlation includes the effect of year of first flight. The year was chosen as 1973 in this study. This yields bare engine thrust to weight ratios just slightly better than with current engines of a similar type. This, combined with some lower efficiencies in the fan and compressor, made the engines of this study slightly heavier than those of reference 4. Thus the usual effect of having high T_{4-cr} lighten the engines should be more pronounced than if the engines were considered to be of advanced light-weight construction.

In addition to the bare engine weight, each engine was assumed to have an installation weight of 3.13 times the corrected total airflow at takeoff. This included such items as inlet, nacelle, and nozzle. This installation weight is based on empirical data for existing high-BPR engines used in large commercial transports. The weight due to suppression of fan noise will be discussed later.

Noise Calculations and Constraints

Noise calculations were made for two measuring points, both of which are specified in Federal Air Regulation Part 36. They were:

(1) Sideline noise measured on the ground at an angle of maximum noise immediately after lift-off on a 0.25-nautical-mile (1520 feet) sideline for three-engine airplanes (0.35-n mi sideline for four-engine airplanes). The point of maximum noise would be after the aircraft had reached an altitude where ground attenuation was zero and fuselage engine masking was diminished.

(2) Approach noise, when the airplane is one nautical-mile from the runway threshold, measured on the ground directly under the glide path at the angle of maximum noise. The airplanes of this study were assumed to be at an altitude of 370 feet at this measuring station.

For the airplanes with TOGW's of interest, FAR Part 36 specifies a noise limit of 106 EPNdB for both of the above points. A third measurement specified by this regulation should be made at a point 3.5 nautical miles from the start of takeoff roll on the extended runway centerline. This noise measurement was ignored in this study because it is felt that little difficulty will be involved in meeting this goal. The reasons for this optimism are explained in detail in appendix B.

Total perceived noise has two components, jet noise from two jet streams and fan turbomachinery noise. The jet noise was calculated by the standard methods described by the Society of Automotive Engineers in references 7 and 8. Fan turbomachinery noise was considered to be a function of FPR and number of stages as shown in reference 9. However, in this report the noise of a two-stage fan was considered to be only 6 PNdB greater than that of a one-stage fan at any FPR. This is in contrast to references 2, 3, 4, and 9 when the difference was considered to be 8 PNdB. This neglects the possible multiple pure tones effect of the high speed one-stage fan. A spectral distribution for fan machinery noise was assumed based on reference 15. The total perceived noise was obtained by adding the machinery noise and jet noise by octaves as described in reference 7 for the addition of two jet streams noise sources. The basic noise calculation in this report were

made in terms of PNdB. However, the results are given in terms of EPNdB. This conversion was accomplished by subtracting 5 PNdB from the approach noise and nothing from the takeoff sideline noise. This method is approximate and is dependent on the time history of the noise and its pure tones. The time history and pure tones of all the engines were assumed to be the same since the takeoff and approach velocities and altitudes were specified. This result agrees with the methods used by industry in a preliminary study like this.

In this study, attention was concentrated on designing cycles that would minimize the TOGW penalties for a given noise goal. Up to 20 PNdB of fan machinery noise suppression was assumed where necessary. It was assumed that no performance losses occurred as a result of adding suppression materials to the inlet and ducts. The weight of acoustic treatment was accounted for, however, by adding weight to the engines according to a schedule which related weight penalty to amount of suppression.

A more detailed description of the noise, suppression, losses, and weight calculations and assumptions is included in appendix B of this report.

Cycle Optimization with Noise and Thrust Constraints

At each FPR and $T_{4\text{-sls}}$ considered, the effects of BPR and OPR on TOGW were calculated. "Thumbprint" plots were then drawn displaying contours of constant TOGW as functions of BPR and OPR. Sideline jet noise and thrust constraints were laid over this thumbprint and a group of good engines meeting thrust constraints were picked off. The complete noise characteristics of these engines were determined and a system of plotting was devised so that the best of these engines could be determined for any noise goal assumed. A description of the method is included in appendix C.

Cost Estimation

Direct operating cost was computed for the selected engines using the standard ATA formula (ref. 5). It was felt that DOC probably serves as a better comparative index than does TOGW. Uncertainties in airplane pricing at this preliminary stage of development make the computational accuracy of DOC in terms of absolute numbers somewhat doubtful. However, the relative merits of the airplanes studied can be compared on a DOC basis. In this study, airframes were assumed to cost \$72 per pound (based on data from ref. 5 for current airplanes). Acoustic suppression for turbomachinery noise was also assumed to cost \$72 per pound. Engine price was assumed to be a function of sea-level-static corrected airflow and was computed as follows,

$$C_{eng} = 1.2\times10^{6}\left[\frac{\left(W_a\sqrt{\theta_1}/\delta_1\right)_{sls}}{1300}\right]^{0.35}$$

This cost is based on empirical data adjusted to reflect the typical cost of a high-BPR turbofan such as those used to power the new wide-body trijets. In all the DOC calculations, the domestic economic ground rules of reference 5 were used.

RESULTS AND DISCUSSION

Cycle Optimization with Fixed Range and Payload

"Thumbprint" performance plots. - Thumbprint plots, such as shown in figures 9(a) to (c), represent the performance of as many as one hundred or more different engines. Looking at figure 9(a), for example, $T_{4\text{-}cr}$ was fixed at 2200° F, $T_{4\text{-}sls}$ was fixed at 2300° F, FPR_{cr} was set at 1.90, but OPR_{cr} was varied from 20 to 44 and BPR_{cr} was varied from 1 to 8. Each combination of these engine parameters represents a point on the plot. Using the techniques described in appendix B of this report, contours of constant TOGW were drawn as well as lines of constant sideline jet noise and constant $(F_N/TOGW)_{sls}$.

For these T_4's and a FPR of 1.90 the lowest TOGW that can be attained is 338 845 pounds at the center point. It can be seen that the engine at this point would have a BPR_{cr} of 3.2, an OPR of 33 and a sideline jet noise of about 113 PNdB. This point would not be acceptable from the standpoint of noise since FAR Part-36 specifies that the noise be a maximum of 106 EPNdB. However, this point is above the line of $(F_N/TOGW)_{sls} = 0.24$ which means that it will probably be acceptable from the standpoint of takeoff thrust.

The engines represented by points above the center point all exceed the $(F_N/TOGW)_{sls}$ minimum of 0.24. Also, the trend for sideline jet noise to be reduced as the BPR_{cr} is increased is obvious. However, as the contours of constant TOGW indicate, any move away from the center point causes some penalty in TOGW. For example, an engine having a BPR_{cr} of 5.0 and a OPR_{cr} of 30 would have a sideline jet noise of only 96 PNdB but the TOGW would be increased to about 343 000 pounds. In this study, these thumbprint plots were used to find promising engines to be examined in more detail. This procedure of selecting good engines from a thumbprint plot is described in appendix B.

At a FPR_{cr} of 1.90, three thumbprint plots were used. One was needed for each of the three $T_{4\text{-}sls}$ studied (i.e., 2300°, 2650°, and 3000° F). These are the figures 9(a) to (c). Examining the three thumbprints in order of increasing $T_{4\text{-}sls}$, several things became apparent. The most obvious is that a $T_{4\text{-}sls}$ of 2650° F (fig. 9(b)) yields the lowest TOGW. A second factor is that as $T_{4\text{-}sls}$ is increased, the best engine cycle (represented by the center circle) creates less sideline jet noise. Another factor is the very noticeable trend for the best engine to have an increasing BPR_{cr} and OPR_{cr} as $T_{4\text{-}sls}$ is increased. A final observation is that it becomes increasingly easier to meet a $(F_N/TOGW)_{sls} = 0.24$ limit as $T_{4\text{-}sls}$ is increased. The other symbols will be explained and used in appendix C.

Figures 10(a) to (c) are for engines with the same $T_{4\text{-}sls}$ values as in figure 9(a) to (c). However, a FPR_{cr} of 2.25 (two-stage fan) has been used in figure 10. The same trends that were shown for a FPR_{cr} of 1.9 (fig. 9(a) to (c)) are again obvious at an FPR of 2.25. However, a comparison between figures 9 and 10 at any $T_{4\text{-}sls}$ shows that the engines

with the FPR_{cr} of 2.25 have lower TOGW for the best engine and lower sideline jet noise. Also obvious is the fact that in figure 10, the best engines are closer to the 0.24 thrust-to-weight minimum than the best engines in figure 9. These are the same trends shown in references 2 to 4.

Comparison in terms of TOGW. - After a complete cycle optimization and noise evaluation was performed, as described in appendix B, the trends in TOGW versus changing $T_{4\text{-sls}}$ were plotted in figure 11. The TOGW's shown in figure 11 represent the best TOGW that can be achieved for several noise goals and for two cruise FPR's. Disregarding noise the best engine of those studied would have an FPR_{cr} of 2.25 and a $T_{4\text{-sls}}$ of 2650° F. This is the point used as a reference point in this report. It corresponds to a TOGW of 338 171 pounds.

According to figure 11, TOGW increases about 1.0 percent at 2300° and 3000° F, for engines with a FPR_{cr} of 2.25 and no noise goal, compared to the reference case. If a noise goal of 106 EPNdB is desired, an additional one percent penalty is added at all $T_{4\text{-sls}}$'s considered. If the noise goal is 101 EPNdB, still another half percent TOGW penalty is added at all $T_{4\text{-sls}}$'s. The minimum TOGW at all these noise goals seem to be around a $T_{4\text{-sls}}$ of 2650° F. At this temperature, the penalty in TOGW is only 1.5 percent to meet a noise goal of 101 EPNdB (FAR 36 minus 5 EPNdB). Lower noise goals will be discussed later.

As was mentioned earlier, if the FPR_{cr} is reduced to 1.90, there is a penalty in TOGW compared to the reference engine with a FPR_{cr} of 2.25. This can be seen in figure 11 also. With no noise goal, the best cycle using a FPR_{cr} of 1.90 still has a TOGW penalty of about 5.8 percent at a $T_{4\text{-sls}}$ of 2650° F compared to the reference case. At a $T_{4\text{-sls}}$ of 2300° F the penalty is 6 percent and at 3000° F it is 6.8 percent. Looking at all the curves for an FPR_{cr} of 1.9, it would seem that the minimum TOGW occurs at about a $T_{4\text{-sls}}$ of 2650° F regardless of the noise goal. At a noise goal of 91 EPNdB (FAR 36 minus 15 EPNdB), the penalty in TOGW is 9.3 percent, with respect to the reference case.

Comparison in terms of DOC. - With only a few minor exceptions the trends and even the actual percent penalties in terms of DOC are the same as in terms of TOGW. This can be seen by a comparison of figures 11 and 12. When considering DOC (fig. 12), the optimum $T_{4\text{-sls}}$ would appear to be about 2600° to 2700° F regardless of the FPR_{cr} or the noise goal. One exception in the likeness of trends is that the buckets in the curves of DOC are not as pronounced as they were in terms of TOGW. In general, this means there is not as much of a penalty in DOC if you miss the optimum $T_{4\text{-sls}}$ as there is in terms of TOGW. Another minor exception is that for engines with a FPR_{cr} of 1.90 and no noise restrictions, increasing $T_{4\text{-sls}}$ seems to always increase DOC (within the $T_{4\text{-sls}}$ limits studied). The DOC at the reference point in figure 12 is 0.545 cents per statute seat mile.

No one doubts the fact that reductions in turbine cooling bleed are advantageous at any given $T_{4\text{-sls}}$. However, once a certain level of cooling technology has been reached (in this report it was assumed to be full-coverage film) the desirability of high T_4's should be examined. This report does this by fixing the engine weight and turbine cooling technology at some specific level. The conclusions that can be reached from these two figures are simple. Increasing $T_{4\text{-sls}}$ beyond 2300° F cannot improve either TOGW or DOC more than $1\frac{1}{2}$ percent. The greatest of these improvements would occur at a $T_{4\text{-sls}}$ between 2600° and 2700° F. Further increases in $T_{4\text{-sls}}$ only worsen TOGW and DOC. Thus, while it is generally accepted that reducing the cooling bleed through advanced technology is good, there seems to be no such good reason to increase $T_{4\text{-sls}}$ beyond 2650° F if you assume full coverage film cooling for the turbines.

Optimum cycle parameters. - The method by which the optimum cycle is found is described in appendix B. The optimum engine cycle parameters, for the engines discussed in figures 11 and 12, are given in figure 13(a). There are 12 parts to figure 13. They are rather simple and do not require a great deal of explanation. They are discussed in order.

Figure 13(a) is a plot of OPR_{cr} versus $T_{4\text{-sls}}$ for a FPR_{cr} of 1.90. The unsuppressed engines have OPR's from 33 to 40 depending on $T_{4\text{-sls}}$. The higher $T_{4\text{-sls}}$'s correspond to the higher OPR's.

As the noise goal is lowered the OPR tends to decrease also.

In figure 13(b), BPR_{cr} is seen to increase with $T_{4\text{-sls}}$ at a given noise goal. It also increases as the noise goals are lowered. These trends are the natural result of trying to balance the cycle so that one of the jet streams will not create much more or less noise than the other while still maintaining an acceptable level of $(F_N/W_a)_{cr}$. Figures 13(c) and (d) show the same trends for a FPR_{cr} of 2.25.

Both FPR_{cr}'s are considered in figures 13(e) and (f). In 13(e) maximum engine diameter is plotted versus $T_{4\text{-sls}}$. The single-stage fan engines ($FPR_{cr} = 1.90$) display a trend to increase in size quite a bit as the noise goal is increased. This is due to the increasing engine airflow at sea-level-static ($W_{a\text{-sls}}$) as shown in figure 13(f). Depending on the noise goal, increasing $T_{4\text{-sls}}$ can either increase or decrease the engine diameter and likewise the engine $W_{a\text{-sls}}$. However, the trend seems to be for $W_{a\text{-sls}}$ to increase with $T_{4\text{-sls}}$ at high noise goals (i.e., 106 EPNdB) and to remain almost constant at low noise goals (i.e., 91 EPNdB). The two-stage fan ($FPR_{cr} = 2.25$) enjoys a smaller diameter and airflow than the one-stage fan at all $T_{4\text{-sls}}$ for equal noise goals. This tends to reduce the drag penalty for the two-stage fans compared to the one-stage fans.

As discussed in the METHOD OF ANALYSIS, in order to determine the correct amount of turbine cooling bleed, the number of turbine stages had to be determined. It was always assumed that the high-pressure turbine required only one stage. The number of stages in the low-pressure turbine did vary over a large range, however. Figure 13(g) shows the range of low-pressure turbine stages required by all of the optimum engines regardless of the FPR_{cr}. Two or three stages were required at a $T_{4\text{-sls}}$ of 2300° F, three or four at 2650° F, and five or six at 3000° F.

The turbine cooling bleed calculated for the optimum engines falls within the bands shown in figure 13(h). The stator always required less cooling than the rotors at any given gas temperature because the blade bulk metal temperature of the stators was allowed to be 2000° F compared to 1650° F for the rotors. The high-pressure turbine rotor

(HP rotor) received most of the cooling air. At a $T_{4\text{-sls}}$ of 2300° F if received a β of about $2\frac{1}{2}$ percent which was all of the cooling flow. At a $T_{4\text{-sls}}$ of 3000° F the HP rotor received a β of 7 to 8 percent. The first LP stator received a β of 1/4 percent and the rest of the low pressure turbine received a β of 4 to 5 percent. Of this 4 to 5 percent, all of it went to the LP rotor and none to the following stators. In fact, none of the LP stators except the first one ever received any cooling air. The total chargeable bleed is the sum of the parts. Total β ranged from about $2\frac{1}{2}$ percent at a $T_{4\text{-sls}}$ of 2300° F to a β of 12 to 13 percent at a $T_{4\text{-sls}}$ of 3000° F.

Even though the high temperature engines required more stages in the turbine and a greater amount of cooling flow, the design turbine efficiencies of both turbines was fixed at all T_4 values. The extra stages and increased cooling flow requirements should have decreased the turbine efficiency. Thus the high temperature engines should probably appear worse than they already do.

The next two figures should be discussed together. Figure 13(i) is the weight penalty due to suppression of fan machinery noise and figure 13(j) is the actual suppression that was required. As described in appendix A, the weight of the suppression material was calculated as a function of actual suppression required and engine diameter as shown in figure 13(e). The weight penalty ranged from as little as 50 pounds (for an engine with a FPR_{cr} of 1.9, $T_{4\text{-sls}}$ of 3000° F, and noise goal of 106 EPNdB) to as much as 480 pounds (for an engine with a FPR_{cr} of 1.9, $T_{4\text{-sls}}$ of 2300° or 3000° F, and a noise goal of 91 EPNdB).

The suppression shown in figure 13(j) is limited to 20 PNdB for practical reasons discussed in appendix A. To meet the FAR-36 goal of 106 EPNdB with a one-stage fan requires only $2\frac{1}{2}$ to 5 PNdB suppression. This is easily within the state of the art. To make a goal of 96 EPNdB (FAR 36 minus 10 EPNdB) requires 15 PNdB of suppression and a goal of 91 EPNdB requires 20 PNdB suppression. A two-stage fan engine ($FPR_{cr} = 2.25$) requires even more suppression than a one-stage fan to meet a given noise goal. This is due in part to the delta of 6 PNdB between a one and two-stage fan and in part to the higher

FPR_{cr} used for the two-stage fan in this report. These points are discussed in the METHOD OF ANALYSIS section and appendix A.

In figure 13(k), $(F_N/TOGW)_{sls}$ is plotted versus $T_{4\text{-}sls}$ for both FPR_{cr}'s at all the noise goals considered. The two-stage fan (FPR_{cr} = 2.25) has a $(F_N/TOGW)_{sls}$ that remains constant at about 0.25 for all $T_{4\text{-}sls}$'s and all noise goals. This is about the minimum acceptable level of 0.24. The $(F_N/TOGW)_{sls}$ for the one-stage fans (FPR_{cr} = 1.9) are somewhat better. They run from 0.270 to 0.287 at noise goals from 106 to 91 EPNdB. The lower noise goals have the higher values of $(F_N/TOGW)_{sls}$. Any of these engines should provide enough F_N at takeoff so that the aircraft can reach a point where the community noise goal at 3.5 miles from start of takeoff roll will be met.

Figure 13(l) shows the ratio of sea-level-static thrust to base engine weight for the one- and two-stage optimum engines. Regardless of the FPR_{cr}, the noise goal, or the $T_{4\text{-}sls}$, the $(F_N)_{sls}$/base engine weight remains between 6 and 7. There is a slight trend for high T_4's to increase the ratio. This is a benefit which high T_4 engines generally enjoy. The noise goals do seem to have a detrimental effect on the ratio if they are pushed to low enough levels. As was intended the ratios are in the same range as for the General Electric CF6-50 which has a $(F_N)_{sls}$/base engine weight ratio of 6.30. These fairly heavy engines should have allowed any benefits of high T_4 to show up in the results.

Tradeoffs of TOGW versus noise. - Figure 14 summarizes the trades in terms of TOGW, noise, suppression, FPR, and advances in technology for engines with a $T_{4\text{-}sls}$ of 2650° F. For reference, a second scale was added to show the noise goals with respect to FAR-36.

For the optimum unsuppressed engine with a FPR_{cr} of 2.25, the noise generated is 122 PNdB. This is the solid triangle point. This noise value is dominated by the approach conditions so that when the previously mentioned conversion is made to EPNdB, the point shifts to 117 EPNdB. This is the reference point. Following the line attached to this point up and to the left, a circled point is reached. This point represents a noise goal of 103.5 EPNdB at a TOGW penalty of 1.2 percent. The machinery suppression required at this point is 15 PNdB

as denoted by the symbol. With today's capabilities, this is about the lowest noise goal that can be obtained by an engine with this FPR_{cr} without very serious increases in TOGW. If 20 PNdB of suppression is postulated for the future, the square point can be reached without much additional penalty. The noise goal would be 100 EPNdB at a TOGW penalty of 1.7 percent. This point was reached not only by the addition of suppression but by re-optimizing the cycle. Further cycle re-optimizing at even lower noise goals was done with the suppression level fixed at 20 PNdB. The TOGW penalties for noise reductions below 100 EPNdB are obviously very serious.

If it is postulated that through advanced technology sometime in the future the unsuppressed optimum engine has a reduction in machinery noise at the source of 5 PNdB, the triangle point moves from 117 to 112.5 EPNdB. This indicates that the noise is machinery source dominated at this point. Following the curve attached to this point it can be seen that a noise goal of 100 EPNdB can be met for a 1 percent TOGW penalty with 15 PNdB of suppression. If 20 PNdB of suppression was available, a slight cycle change would give a noise goal of 97 EPNdB at a TOGW penalty of 1.8 percent (the square point). Further cycle changes could be made with the suppression fixed at 20 PNdB (the dashed line). These would result in small noise reductions and large TOGW penalties.

If a family of engines with a FPR_{cr} of 1.90 are considered, the curves in the upper portion of the figure results. The optimum unsuppressed engine could meet a noise goal of 115 PNdB at a TOGW penalty of 5.7 percent (the solid triangle). Correcting to EPNdB moves the point to 110 EPNdB. The circled point on this line indicates a noise goal of 98 EPNdB can be met at a TOGW penalty of 7.4 percent with only 15 PNdB of suppression. This should be within the state-of-the-art. If advanced technology provides 20 PNdB of suppression, the square point may be reached by a slight change in the cycle. This would yield a noise goal of 94 EPNdB at a TOGW penalty of 8.1 percent. Any further reductions in noise at a constant 20-dB suppression level (dashed line) will result in large TOGW penalties even though the engines are re-optimized.

If future advances in technology provide a fan that is quieter at the source by 5 PNdB, the optimum unsuppressed noise would be 105 EPNdB (the triangle point). This shift from 110 to 105 EPNdB indicates that the noise is machinery noise dominated. Following this line up to the circled point indicates that a noise goal of 94 EPNdB can again be met but with only 15 PNdB of suppression. The TOGW penalty would be 7.7 percent. If 20 PNdB of suppression is postulated then a noise goal of 90 EPNdB can be met at a TOGW penalty of 9.1 percent (the square point). Any further noise reductions would be expensive in terms of TOGW if the suppression is fixed at 20 EPNdB (dashed line). This is because the cycle would have to change, moving quickly away from optimum as the noise is reduced.

From this figure it can be seen that increasing the suppression available from 15 to 20 PNdB could yield noise reductions of about 3 to 4 PNdB if the cycle is changed somewhat also. The penalties would be about 1/2 to 1 percent in TOGW. These penalties could be greater if the extra 5 PNdB of suppression is as hard to obtain as it appears to be today.

The other method for reducing noise is to reduce machinery noise at the source assuming constant suppression. A 5 PNdB reduction at the source would yield noise reductions of 3 to 4 PNdB. Comparing any two circled points or squared points in figure 14 at a given FPR_{cr} indicates that the TOGW penalty for this noise reduction may range from none to $1\frac{1}{2}$ percent. The penalties could be larger if the source noise reduction technique causes an engine weight penalty. None was assumed in this report.

It would appear that a noise goal of 103.5 EPNdB (FAR 36 minus 2.5 dB) could be met by an engine with a FPR_{cr} of 2.25 using today's technology. The TOGW penalty would be about 1.2 percent. With advanced technology a noise goal of 97 EPNdB (FAR 36 - 9 dB) may be met with an additional TOGW penalty of at least 0.6 percent.

If the engines had a FPR_{cr} of 1.90, a noise goal of 98 EPNdB (FAR-36 minus 8 dB) can be met for a TOGW penalty of 1.7 percent compared to the optimum unsuppressed engine at the same FPR_{cr} or

7.4 percent with respect to the reference engine. Advanced technology may be able to lower the noise goal to 90 EPNdB (FAR-36 minus 16 dB). The TOGW penalty would be 3.5 percent compared to the optimum unsuppressed engine at the same FPR_{cr} or 9.1 percent with respect to the reference.

CONCLUDING REMARKS

A parametric study was made of a group of separate-flow-exhaust turbofan engines for use in an advanced-technology transport designed to cruise at Mach 0.98. Initial cruise altitude was 40 000 feet, total range was 3000 nautical miles and the payload was 60 000 pounds (300 passengers). The airplane was assumed to have 3 aft-mounted engines of slightly advanced weight technology. An advanced turbine cooling scheme was assumed (full coverage film) and the cooling for each stage of the turbine was calculated. Turbine-rotor-inlet-temperature of 2300°, 2650°, and 3000° F were examined at sea-level-static standard day conditions. The optimum turbine-inlet-temperature at cruise was always 100° F less than the sea-level-static value, that is, the highest allowed in the study. Combined jet and fan machinery noise calculations were made for selected cycles at both the sideline and approach measuring stations specified in FAR Part 36. Varying amounts of acoustic treatment were applied to the inlet, duct and nacelle to obtain certain levels of turbomachinery noise.

Fan pressure ratios (FPR) of 1.90 (one-stage fan) and 2.25 (two-stage fan) were used. Engine parameters of bypass ratio and compressor pressure ratio were optimized for each FPR and turbine-inlet-temperature combination. Noise goals as low as 86 EPNdB (FAR-36 minus 20 EPNdB) were examined. The optimum engines were defined at several levels of noise so tradeoffs between takeoff-gross-weight (TOGW) and noise could be seen.

It was found that if the noise goal was equal to or less than 106 EPNdB (FAR-36), the optimum sea-level-static turbine-inlet-temperature ($T_{4\text{-sls}}$) was about 2650° F. This was true whether the figure of merit

was TOGW or direct operating cost (DOC). However, the figure of merit was rather insensitive to T_4 within $\pm 100^{\circ}$ F. TOGW or DOC was only about 1 percent worse if the lowest value of $T_{4\text{-sls}}$ studied was used (2300° F) or the highest value studied was used (3000° F) rather than the optimum 2650° F. This lack of benefit of high T_4 was found despite several assumptions that should have favored high T_4 (heavy engines, advanced turbine cooling method, and no penalties in turbine efficiency with more turbine stages and increased turbine cooling bleed).

If the $T_{4\text{-sls}}$ was fixed at 2650° F, it was found that a two-stage-fan with a FPR of 2.25 could meet a noise goal of 103.5 EPNdB (FAR-36 minus 2.5 EPNdB) with today's noise suppression techniques. This would cause a penalty in TOGW of about 1 percent. With some advances in noise suppression techniques the noise could be lessened another 7 EPNdB at the expense of another 1 percent in TOGW. Any reductions in noise beyond this were estimated to be very costly in terms of TOGW or DOC.

At the same turbine-inlet-temperature, a single-stage fan with an FPR_{cr} of 1.90 was less of a noise problem. However, the best engine without any noise suppression was 5.7 percent heavier in TOGW than the best two-stage fan engine. A noise goal of 96 EPNdB (FAR Part 36 minus 10 EPNdB) could be met with the single-stage fan with today's technology in noise suppression. The penalty over the unsuppressed case would be an additional 2.0 percent in TOGW. The noise goal could be lowered another 6 EPNdB if some advances were made in source noise reduction and suppression techniques. This would cost an additional 1.5 percent in TOGW. Any reductions in noise beyond this were estimated to be very costly in terms of TOGW or DOC.

APPENDIX A

COOLING BLEED FLOW CALCULATION

In order to calculate the total cooling bleed for the two turbines, the number of stages in each turbine must be determined as well as the thermodynamic conditions at each stage.

The high-pressure turbine was assumed to have one stator and one rotor. The cooling flow for the stator is not calculated since it would be included in the combustor airflow. After the stator cooling flow has re-entered the primary stream and mixed with it, the conditions at the rotor inlet are determined. This is station 4 in our nominclature. Thus T_4 would be turbine-rotor-inlet-temperature and any stator cooling bleed prior to station 4 would be called non-chargeable to the cycle.

The cooling bleed for the high-pressure turbine rotor was calculated by the following method. First φ was calculated where

$$\varphi = \frac{T_{gi} - T_m}{T_{gi} - T_{ci}} \tag{A1}$$

T_{gi} is the total temperature of the gas at the face of the stage and T_{ci} is the total temperature of the cooling air (compressor exit temperature). T_m is the average bulk metal temperature of the blades being considered. T_m was 1650° F for all rotors and 2000° F for all stators. Once φ was calculated, the curve in figure 6 was used to find the coolant flow ratio W_c/W_{gi}. This ratio was increased by one-third to account for shroud cooling and losses. The curve in figure 6 was taken from reference 11. The curve is based on laboratory tests of blades using full-film coverage for cooling. The blades were made with advanced fabrication techniques.

In the low-pressure turbine the number of stages had to be calculated in order to calculate the bleed for any stage that needed it. The following discussion is a derivation of the equation used to calculate the number of stages.

A schedule of fan tip speed ($V_{fan\text{-}tip}$) was estimated versus FPR. The curve is based on data from reference 10. It is a linear approximation tangent to the curve in reference 10 for a fan blade loading of 0.3 at a $V_{fan\text{-}tip}$ of 1900 ft/sec. The derivation follows.

ω is the velocity in radians/sec

$$V_{fan\text{-}tip} = \omega \times D_{ia\text{-}fan}/2 \tag{A2}$$

$$\omega = 2\, V_{fan\text{-}tip}/D_{ia\text{-}fan} \tag{A3}$$

$$W_1/W_{2,\,core} = 1 + BPR = \text{ratio of total airflow to core airflow} \tag{A4}$$

The following equations have to do with the turbine exit station.

$$W_{g,\,6}/W_{2,\,core} = 1 + FA_4(1 - Bleed_{total}) = \text{ratio of gas} \tag{A5}$$

flow at station 6 to core airflow

$$U_m = \text{mean rotational velocity of turbine} = D_m \times \omega/2 \tag{A6}$$

where D_m = mean diameter of turbine blades.

$$A_6 = 0.64\pi\, D_t^2/4 \quad \text{if} \quad D_h/D_t = 0.6 = \text{turbine hub to tip ratio} \tag{A7}$$

$$D_m = 0.8\, D_t \tag{A8}$$

$$A_6 = \pi\, D_m^2/4 \tag{A9}$$

$$W_{g,\,6}/W_{2,\,core} = \rho_6 A_6 V_6 = \sqrt{\gamma_6\, g/R_6 t_6}\; \pi\, D_m^2 M_6 p_6/4 \tag{A10}$$

where

ρ density

A area

V velocity

γ ratio of specific heats

g gravitational constant

R gas constant

t static temperature

M Mach number

p static pressure

The turbine work parameter λ is defined as follows. It was assumed to be 0.4 in all cases.

$$\lambda_{stage} = N\, U_m^2/gJ\, \Delta H = 0.4 \tag{A11}$$

where

N number of stages

J mechanical equivalent of heat = 778 ft-lbs/Btu

ΔH change in enthalpy from stations 5 to 6

$$N = (0.4gJ\, \Delta H_{5,6}/V_{fan\text{-}tip}^2)(D_{ia\text{-}fan}/D_m)^2 \tag{A12}$$

Letting equations (A5) and (A10) equal and solving for D_m^2 yields:

$$D_m^2 = \left[1 + FA_4(1 + Bleed_{total})\right] \times 4 \times \sqrt{R_6 t_6/\gamma_6 g}\,/(\pi M_6 p_6) \tag{A13}$$

The following equations have to do with the fan face station.

$$A_1 = 0.88\pi\, D_{ia\text{-}fan}^2/4 \tag{A14}$$

if

$$\left(D_h/D_t\right)_{fan} = 0.35, \text{ hub to tip ratio of fan} \tag{A15}$$

$$W_1/W_{2,core} = 0.88\pi\, D_{ia\text{-}fan}^2 M_1 p_1 \sqrt{\gamma_1 g/R_1 t_1}\,/4 \tag{A16}$$

Solving for $D^2_{ia\text{-}fan}$

$$D^2_{ia\text{-}fan} = (1 + BPR)4\sqrt{R_1 t_1/\gamma_1 g}\Big/(0.88\pi M_1 p_1) \tag{A17}$$

Dividing equation (A17) by equation (A13) yields

$$\frac{D_{ia\text{-}fan}}{D_m}^2 = (1 + BPR)(P_6/P_1)\sqrt{T_1/T_6}\Big/\left[1 + FA_4(1 + Bleed_{total})\right]0.88 \tag{A18}$$

if $M_1 \cong M_6$ and if $\gamma_1 \cong \gamma_6$

Substituting equation (A18) into equation (A12) yields

$$N = \frac{9660(1 + BPR)(P_6/P_1)\,\Delta H_{5,6}}{\left[1 + FA_4(1 - Bleed_{total})\right]V^2_{fan\text{-}tip}\sqrt{T_6/T_1}} \tag{A19}$$

when N is the number of stages. The ΔH across each low pressure turbine stage was assumed to be the same as was the ΔT.

Once N was determined then ΔT per stage was estimated to be

$$\Delta T_{stage} = (T_5 - T_6)/N \tag{A20}$$

T_5 and T_6 are known from the cycle calculation where the low pressure turbine is treated as a whole. Now using figure 6 the bleed for each stage of the low pressure turbine is calculated just as it was for the high pressure turbine rotor. The bleeds as summed to a total bleed ($Bleed_{total}$) which is used in the equations just shown and in the cycle calculations. If the $Bleed_{total}$ calculated does not equal the $Bleed_{total}$ used in the equations, the entire process is reported as necessary until they are equal.

APPENDIX B

NOISE CONSTRAINTS

Noise calculations were made for two measuring points, both of which are specified in Federal Air Regulation Part 36. They were:

(1) Sideline noise measured on the ground at the angle of maximum noise immediately after lift-off on a 0.25-nautical-mile (1520-ft) sideline for three-engine airplanes (0.35-n mi sideline for four-engine airplanes). The point of maximum noise would be after the aircraft reached an altitude where ground attenuation was zero and fuselage engine masking was diminished.

(2) Approach noise, when the airplane is one nautical mile from the runway threshold, measured on the ground directly under the glide path at the angle of maximum noise. The airplanes of this study were assumed to be at an altitude of 370 feet at this measuring station.

For airplanes with TOGW's of interest, FAR Part 36 specifies a noise limit of 106 EPNdB for both of the above measurements. A third measurement specified by this regulation should be made at a point 3.5 nautical miles from the start of takeoff roll on the extended runway centerline. If the airplane altitude at this measuring point exceeds 1000 feet, the thrust may be reduced to that required for a 4 percent climb gradient or to maintain level flight with one engine out, whichever thrust is greater. The noise limit at this measuring station for the TOGW's considered here is 102-104 EPNdB. This noise measurement was ignored in this study because insufficient low-speed aerodynamic data were available to investigate the tradeoffs involved in minimizing noise at this point. The tradeoffs involved are between constant Mach number climb to maximum altitude and maximum acceleration to 1000 feet before thrust is reduced. For the three-engine airplanes which meet a sideline noise goal in this study, it is felt that little difficulty will be involved in meeting the 3.5-mile "takeoff" goal since the sideline noise is measured at 1520 feet. With four-engine airplanes, the 3.5-mile goal might be more difficult to meet, however, because the sideline measurement is specified at 2126 feet and is therefore

easier to meet. The 3.5-mile measurement might thus be more of a constraint for four-engine airplanes.

Total perceived noise has two components - jet noise from the two jet streams and fan turbomachinery noise. Jet noise, measured in PNdB, was calculated by standard methods described by the Society of Automotive Engineers in references 7 and 8. Jet noise is primarily dependent on the exit velocities of the two flow streams, but is also affected by the gas flow rates and the flow areas. These variables were calculated at both Mach 0.23 (152 knots) after lift-off at full thrust and with thrust cut back to the level required during the 3° approach at Mach 0.203 (135 knots). It was assumed that the overall SPL curve of reference 7 plotted against relative jet velocity could be linearly extrapolated on a log scale to velocities below 1000 feet per second (as per data presented in ref. 9).

Fan turbomachinery noise, also measured in PNdB, is a function of many things - for example, spacing between stator and rotor, tip speed, number of stages, fan pressure ratio, thrust, and amount of nacelle acoustic treatment. In this study, it was assumed that the engines would be built with optimum stator-rotor spacing without any inlet guide vanes in order to minimize noise. Curves presented in reference 9 relate machinery perceived noise level to fan pressure ratio at a fixed thrust and distance for both one- and two-stage fans. These curves were scaled from a total airplane net thrust of 90 000 pounds and a measuring-point distance of 1000 feet to both the sideline and approach conditions of this report. In addition to logarithmic thrust and distance-squared scaling, extra air absorption due to a change in slant range (ref. 7) was included. However, in this report, the curve for the two-stage fans was lowered an extra 2 PNdB. The difference between one- and two-stage fans is only 6 PNdB instead of 8 PNdB as in references 2 to 4 and 19. This change is based on the latest estimates of the noise experts at Lewis Research Center but does not include the effects of multiple pure tones. The curves which result for the sideline condition are shown in figure 15(a) for a total airplane net thrust of 114 000 pounds. The curves which result for the approach condition are shown in figure 15(b)

for a total airplane net thrust of 36 000 pounds. These noise levels assume the present state-of-the-art quieting techniques. These thrust levels are typical for airplanes having a TOGW of 386 000 pounds. But when range was fixed at 3000 nautical miles, TOGW was usually less than 386 000 pounds. Therefore it was necessary to correct these turbomachinery noise readings (fig. 15) for the variation in thrust. The sideline noise correction is plotted against total thrust from three engines in figure 16(a). The approach fan turbomachinery noise correction is plotted against TOGW with total thrust as an auxiliary scale in figure 16(b).

In order to determine the total perceived noise from both the jets and the fan turbomachinery, it was necessary to add antilogarithmically the jet and machinery sound pressure levels (SPL) in each octave. (This procedure is described in ref. 7 for the addition of core and fan jet noise.) To do this, it was necessary to assume a spectral distribution of fan turbomachinery SPL as a function of frequency. Figure 17 shows octave SPL (in dB) at a distance of 200 feet that was assumed for all the fans considered in this study. This octave SPL was attenuated for the inverse-square distance effect and the extra-air-absorption effect at distances greater than 200 feet, as described in reference 7. The distance-squared effect is the same for all octaves, but the extra air absorption affects the higher octaves the most. The spectrum shown in figure 17 depicts data obtained from reference 15 for a TF39 fan modified for low noise. It was assumed that the spectral distribution would not change significantly with power setting or acoustic treatment.

To obtain the octave SPL of the fan machinery noise, the perceived noise level in PNdB was first obtained from the curves of figure 15. Corrections from figure 16 were then applied. The amount of attenuation from acoustic treatment, if any, was subtracted. Absolute numbers were then arbitrarily placed on the ordinate scale of figure 17 and the fan machinery perceived noise was computed by summing and manipulating the octave SPL's thus obtained, as described in reference 7. The calculation was repeated by sliding the arbitrary ordinate scale of figure 17 up or down as required in an iterative calculation until the fan

perceived noise thus calculated equaled that read from the curves of figure 15 (as modified by fig. 16 and the application of acoustic treatment). After completing this computerized iteration, machinery octave SPL was added antilogarithmically to the combined jet SPL at each octave. Total perceived noise was obtained by summing and manipulating all the combined octave SPL's (as described in ref. 7).

The basic noise calculations made in this study are in units of PNdB. The FAR Part 36 requirements, however, are stated in terms of EPNdB. The EPNdB scale (where E stands for effective) is a modification of the PNdB scale where a correction is made to account for (1) subjective response to the maximum pure tone and (2) the duration of the noise (ref. 16) heard by the observer. Industry has pretty well agreed that, for the takeoff and approach conditions assumed in this study, EPNdB at takeoff is about the same as PNdB, and that EPNdB during approach is about 5 dB less than PNdB. So in this report the basic unit was EPNdB. This means that 5 dB was subtracted from the total approach noise as calculated in PNdB and discussed thus far in order to convert to EPNdB.

In this study, attention was concentrated on designing cycles that would minimize the TOGW penalties that occur with up to 20 PNdB of turbomachinery acoustic treatment. Noise goals as low as 90.0 EPNdB were obtained with this amount of acoustic treatment. As discussed in the section entitled "Engines," in the METHOD OF ANALYSIS, a 20-PNdB suppression of fan turbomachinery noise is thought to be a somewhat optimistic - although still realistic - goal to strive for. As mentioned in reference 9, it is felt that a 15-PNdB suppression of turbomachinery noise can currently be realized with proper suppressor design. It was assumed in this study that no performance losses occurred as a result of the insertion of splitter rings in the inlet and duct, together with wall lining in the inlet, duct, and nacelle. It is encouraging to note that tests of a 6-foot fan with acoustic treatment which included multiple splitter rings (ref. 17) did not reveal any fan performance losses due to the noise suppressors, within the experimental measurement error.

Duct and inlet wall treatment and an acoustically lined splitter ring inserted in the inlet were found in reference 18 to penalize the weight of a Pratt & Whitney JT3D engine about 370 pounds. Much of this weight penalty is undoubtedly due to structural modification since the lining material by itself is very light. This amount of treatment on the JT3D engines of a DC8 airplane lowered the approach noise about 11 PNdB. The addition of one splitter to the inlet of some of the high BPR engines of this study may not be as effective in reducing approach noise of these engines as it was for the low-BPR JT3D because of the larger inlet diameter-to-sound-wave-length ratio (ref. 19). It was estimated in this study that this type of inlet and duct treatment combined will reduce the fan machinery noise about 10 PNdB. A 15-PNdB reduction, the maximum demonstrated to date, can be attained only by the addition of more splitter rings in the inlet and probably the addition of splitter rings in the duct as well (ref. 20).

In both references 18 and 20, the weight penalties involved more than just treatment weight. There were structural changes to the engine as well. To separate the weight due to treatment and the weight due to structure is impossible from those references alone. However, reference 21 indicates that two splitter rings weigh 150 pounds. To achieve 10 PNdB suppression in a long duct engine, the inlet needs only one ring and the duct and inlet walls must be treated. In this report it was assumed that this could be done for 150 pounds on a 53-inch-diameter engine. Of this, 75 pounds was attributed to the single splitter and the other 75 pounds to the treatment of the duct and inlet walls. When 15 PNdB was required in this study, it was assumed that the extra inlet ring and additional duct treatment weigh 75 pounds for a 53-inch-diameter engine. Since most of the treatment weight is applied near the periphery of the engine, treatment weight was scaled directly with maximum engine diameter in this study. The airplane operating-empty-weight penalty due to turbomachinery noise suppression used in this study is plotted as a straight line (fig. 18) through the origin and these two points at 10 and 15 PNdB of suppression. Engine diameter was adjusted for this plot from 53 inches to the nominal 80-inch size more compatible with high-BPR turbofans.

APPENDIX C

CYCLE OPTIMIZATION TECHNIQUE

Once all of the techniques and assumptions in this report have been computerized, it is not to hard to design and fly a great many engines in just a few minutes of computer time. At the start of the study two FPR's were chosen - 1.9 and 2.25. Three $T_{4\text{-sls}}$'s were also chosen - 2300°, 2650°, and 3000° F. However, the cruise T_4's still had to be decided upon.

First, four different $T_{4\text{-cr}}$ values were assumed, at 100°, 200°, 300°, and 400° F less than the $T_{4\text{-sls}}$. Then BPR_{cr} was varied over a wide range at several fixed values of OPR. Without any consideration of noise at this point, it was easy to see that the engines with a $T_{4\text{-cr}}$ of only 100° F less than $T_{4\text{-sls}}$ were far superior in terms of TOGW. It was also noted at this time that the $(F_N/TOGW)_{sls}$ values of all of these engines were acceptable (>0.24). Thus a delta T_4 of 100° F was decided upon for all $T_{4\text{-sls}}$ values considered and for both FPR's. As in reference 4, this delta T_4 would have probably been greater than 100° F if lower M_{cr}'s or cruise altitudes had been chosen for the study.

Once the optimum delta T_4 of 100° F had been decided upon, the TOGW was plotted versus BPR_{cr} on lines of constant OPR_{cr}. This was done for the six cases of interest, two FPR's at three $T_{4\text{-sls}}$'s. A cross plot of each of these plots on lines of constant TOGW yields the thumbprints already discussed and shown as figures 9(a) to (c) and 10(a) to (c). Overlaid on these six thumbprints are lines of constant sideline jet noise. This was easily calculated in the same computer program since all of the engine exhaust parameters are calculated for each engine at sea-level takeoff conditions. To show that $(F_N/TOGW)_{sls}$ is not a problem, a limiting line of constant $(F_N/TOGW)_{sls} = 0.24$ is shown on each plot. It always falls below the minimum TOGW contour and thus is of no further concern.

In order to illustrate the actual optimization procedure a specific example will be used. The problem given is to find the optimum cycle

if the FPR_{cr} is 1.90, the $T_{4\text{-}sls}$ is 2650^{0} F, and the noise goal is 96 EPNdB.

First, six very good engines are chosen from the thumbprint plot, figure 9(b). These are the designated points, starting with the best cycle represented by the circle. The points are selected by eye and are hopefully on a locus that connects all the points that are tangent between lines of constant sideline jet noise and contours of constant TOGW. These tangent points represent the point of minimum TOGW for a particular sideline jet noise level.

Now that these six engines have been chosen to be examined in more detail, each one is rerun in the computer assuming levels of suppression from 0 to 20 PNdB in steps of 5PNdB. This establishes the TOGW for each level of suppression. The TOGW penalty is due to the suppression weight penalty as previously discussed and shown in figure 18. Takeoff fan machinery noise is calculated for each engine assuming different amounts of suppression. The fan noise and jet noise are then added antilogarithmically, octave-by-octave, to give a total PNdB level. For takeoff it was assumed that PNdB and EPNdB were the same. A curve, figure 19(b), is then plotted showing TOGW versus sideline noise for lines of constant fan noise suppression. All six of the engines are noted in the figure by the symbols. The shaded and unshaded symbols are just to aid the human eye in following the lines of constant suppression.

Next, each of the six engines is run in the component matching deck to determine the proper match point at approach conditions. This establishes the jet noise at approach and the FPR at approach. From figures 15 and 16 the approach fan noise is read and corrected. Assuming varying amounts of suppression ties each engine to a particular TOGW once more. The fan and jet noise are again added as before to get a total PNdB. Then 5 PNdB is subtracted from the total to get EPNdB. This is an approximate method in wide use by industry. Each engine with varying amounts of fan noise suppression has a sideline and approach noise level in EPNdB now and a certain TOGW. At this point figure 19(a) is plotted directly below figure 19(b). With approach and sideline noise tied together by figure 19(a) and TOGW and sideline

noise tied together in figure 19(b), the search for the optimum cycle can begin.

First an area is roped off in figure 19(a) which satisfies a goal of 96 EPNdB. Some point in this area will give the lowest TOGW. The dashed lines are added between symbols to aid the interpolation that is necessary. If the reader spends a few minutes at this time and examines the points labled A, B, C, D, E, and random point F, it should be clear that point D yields the minimum TOGW of any point in the entire area. Some interpolation is necessary to decide exactly what cycle is represented by point D. The conclusion should be that a cycle at point D would have an FPR of 1.9, $T_{4\text{-sls}}$ of 2650° F, an OPR of 34+, a BPR of about 6.8 and require 15 PNdB of suppression. It would make a noise of about 94.7 EPNdB during approach and 96 EPNdB at the sideline during takeoff. This same procedure was used to select every engine at every noise goal.

If a curve is plotted using PNdB instead of EPNdB, the optimization technique is the same as above. However, the 5 PNdB is not subtracted from the approach noise as it was to convert to EPNdB.

REFERENCES

1. Thomas, B. K., Jr.: New Wing Promises Design Breakthrough. Aviation Week and Space Tech., vol. 87, no. 4, July 24, 1967, pp. 25-26.

2. Whitlow, John B., Jr.; Kraft, Gerald A.; and Civinskas, Kestutis C.: Parametric Engine Study for a Mach 0.98 Commercial Air Transport. NASA TM X-52961, 1971.

3. Kraft, Gerald A.; and Whitlow, John B., Jr.: Optimization of Engines for a Mach 0.98 Transport with Low Takeoff and Approach Noise Levels. NASA TM X-67865, 1971.

4. Whitlow, John B., Jr.; and Kraft, Gerald A.: Optimization of Engines for Commercial Air Transports Designed for Cruise Speeds Ranging from Mach 0.90 to 0.98. NASA TM X-67906, 1971.

5. Anon.: Standard Method of Estimating Comparative Direct Operating Costs of Turbine Powered Transport Airplanes. Air Transport Association of Am., Dec. 1967.

6. Cleveland, F. A.: Size Effects in Conventional Aircraft Design. J. Aircraft, vol. 7, no. 6, Nov.-Dec. 1970, pp. 483-511.

7. Anon.: Jet Noise Prediction. Aerospace Information Report 876, SAE, July 10, 1965.

8. Anon.: Definitions and Procedures for Computing the Perceived Noise Level of Aircraft Noise. Aerospace Recommended Practice 865, SAE, Oct. 15, 1964.

9. Kramer, James J.; Chestnutt, David; Krejsa, Eugene A.; Lucas, James G.; and Rice, Edward J.: Noise Reduction. Aircraft Propulsion. NASA SP-259, 1971, pp. 169-209.

10. Hartmann, Melvin J.; Benser, William A.; Hauser, Cavour H.; and Ruggeri, Robert S.: Fan and Compressor Technology. Aircraft Propulsion. NASA SP-259, 1971, pp. 1-36.

11. Livingood, John N. B.; Ellerbrock, Herman H.; and Kaufman, Albert: 1971 NASA Turbine Cooling Research Status Report. NASA TM X-2384, 1971.

12. McKinney, John S.: Simulation of Turbofan Engine. Part I. Description of Method and Balancing Technique. Rep. AFAPL-TR-67-125, pt. 1, Air Force Aero Propulsion Lab., Nov. 1967.

13. McKinney, John S.: Simulation of Turbofan Engine. Part II. User's Manual and Computer Program Listing. Rep. AFAPL-TR-67-125, pt. 2, Air Force Aero Propulsion Lab., Nov. 1967.

14. Gerend, Robert P.; and Roundhill, John P.: Correlation of Gas Turbine Engine Weights and Dimensions. AIAA Paper 70-669, June 1970.

15. Kramer, James J.: Quiet Engine Program Detailed Engine Designs. Progress of NASA Research Relating to Noise Alleviation of Large Subsonic Jet Aircraft. NASA SP-189, 1968, pp. 273-285.

16. McPike, A. L.: Recommended Practices for Use in the Measurement and Evaluation of Aircraft Neighborhood Noise Levels. SAE Paper 650216, Apr. 1965.

17. Rice, Edward J.: Performance of Noise Suppressors for a Full-Scale Fan for Turbofan Engines. NASA TM X-52941, 1971.

18. Pendley, Robert E.: Introduction to McDonnel Douglas Program. NASA Acoustically Treated Nacelle Program. NASA SP-220, 1969, pp. 19-28.

19. Feiler, Charles E.; Rice, Edward J.; and Smith, L. Jack: Performance of Inlet Sound Suppressors. Progress of NASA Research Relating to Noise Alleviation of Large Subsonic Jet Aircraft. NASA SP-189, 1968, pp. 53-62.

20. Atvars, Janis; Mangiarotty, R. A.; and Walker, David Q.: Acoustic Results of 707-320B Airplanes with Acoustically Treated Nacelles. NASA Acoustically Treated Nacelle Program. NASA SP-220, 1969, pp. 95-108.

21. Pendley, Robert E.: Design Concepts. Progress of NASA Research Relating to Noise Alleviation of Large Subsonic Jet Aircraft. NASA SP-189, 1968, pp. 113-129.

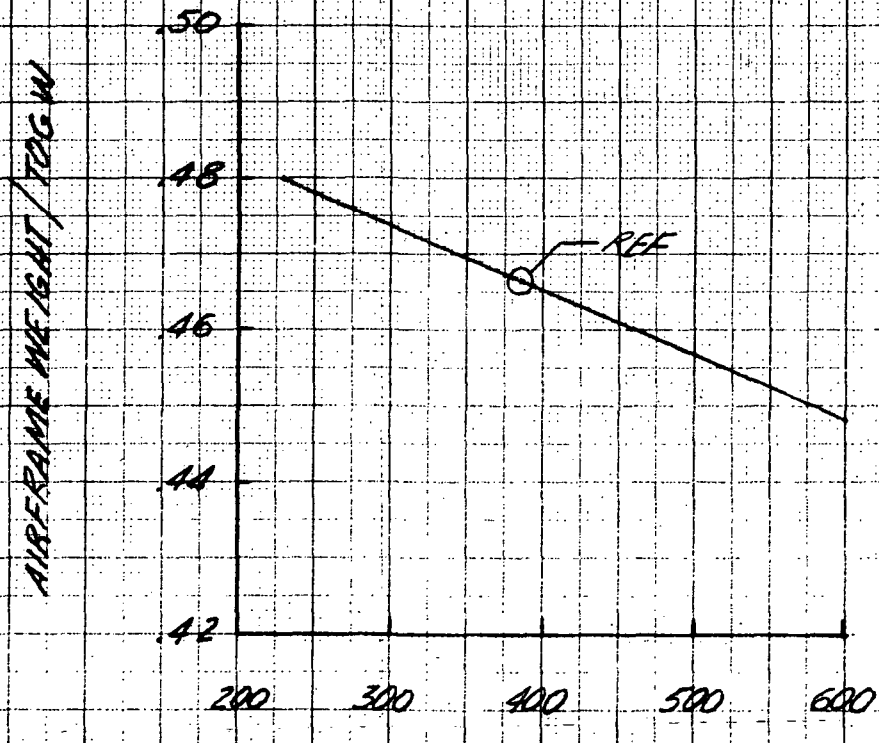

FIGURE 1.- AIRFRAME WEIGHT FRACTION. FUSELAGE DIMENSIONS FIXED, TAKEOFF WINGLOADING FIXED.

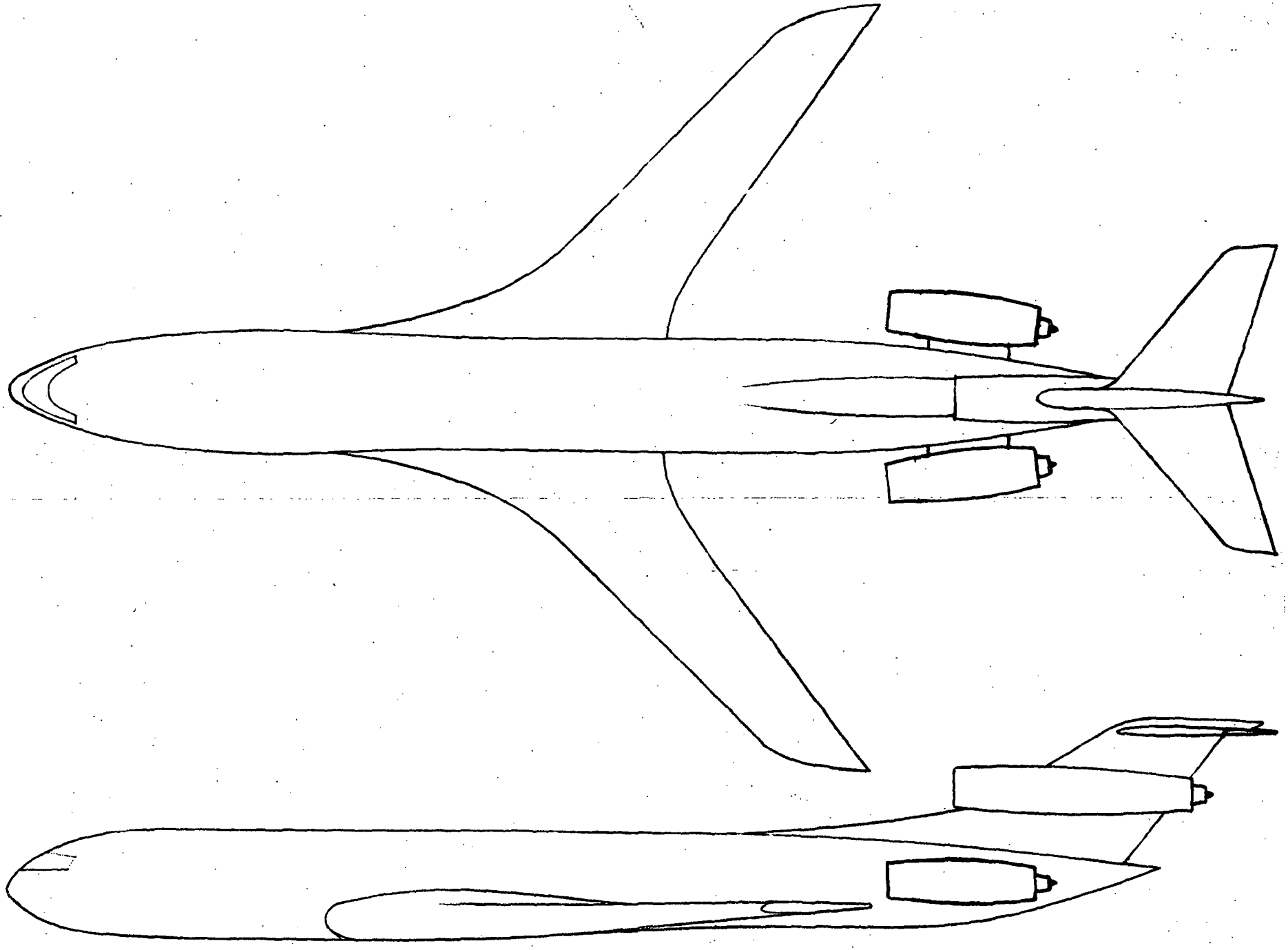

FIGURE 2. — SKETCH OF CONCEPTUAL ADVANCED TRI-JET TRANSPORT.

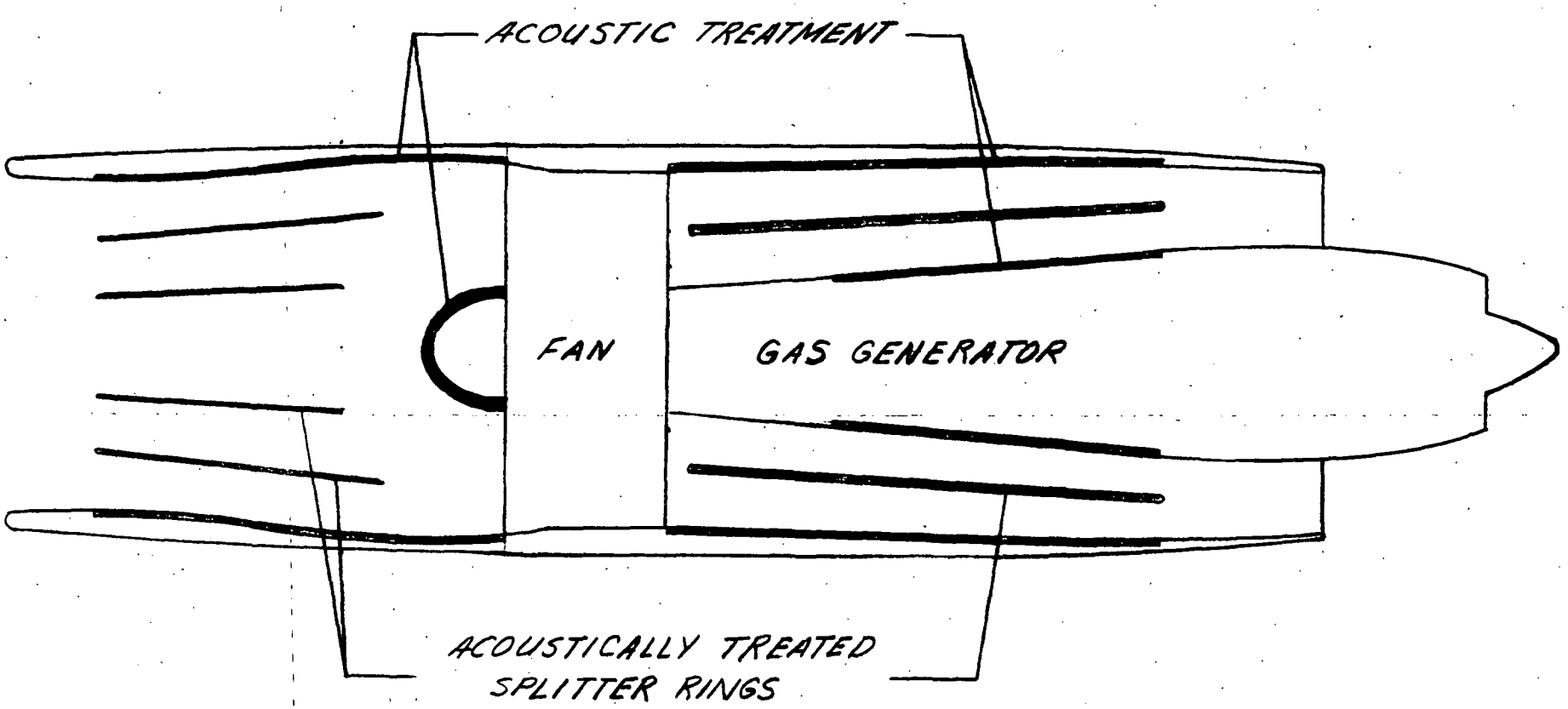

FIGURE 3.- SKETCH OF TURBOFAN ENGINE WITH ACOUSTIC TREATMENT

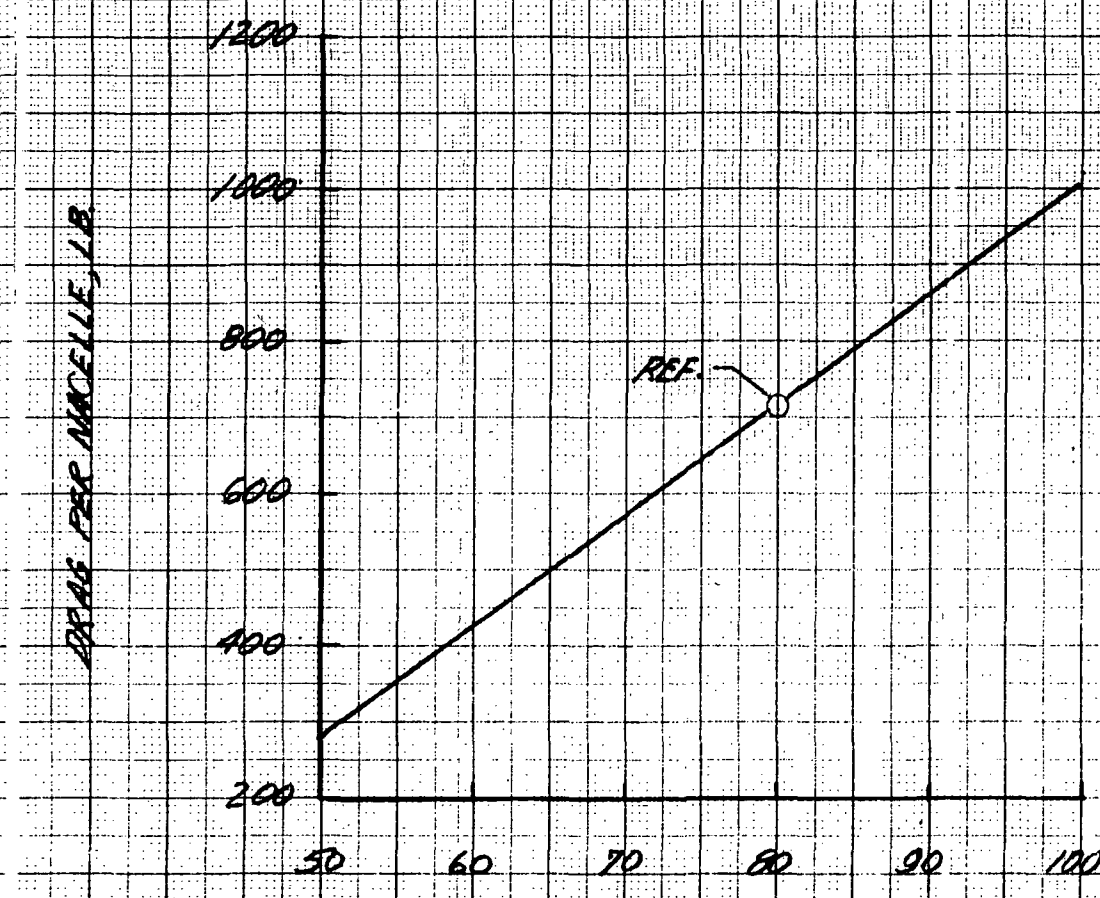

FIGURE 4.- NACELLE DRAG RELATED TO ENGINE MAXIMUM DIAMETER. CRUISE MACH NUMBER, 0.98.

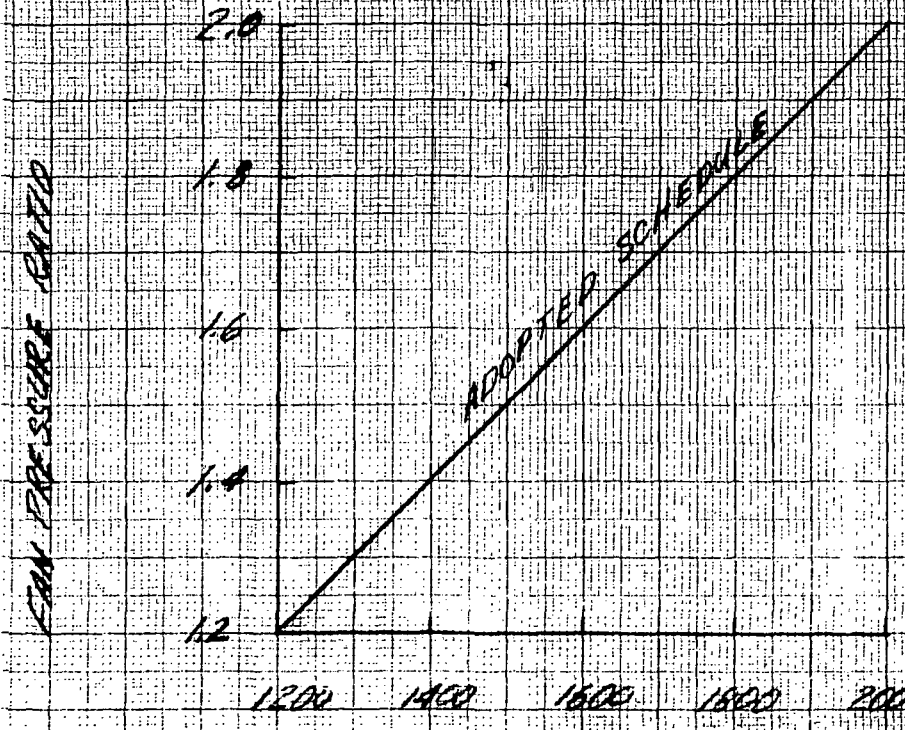

FIGURE 5.- FAN TIP SPEED FOR ONE STAGE FANS.

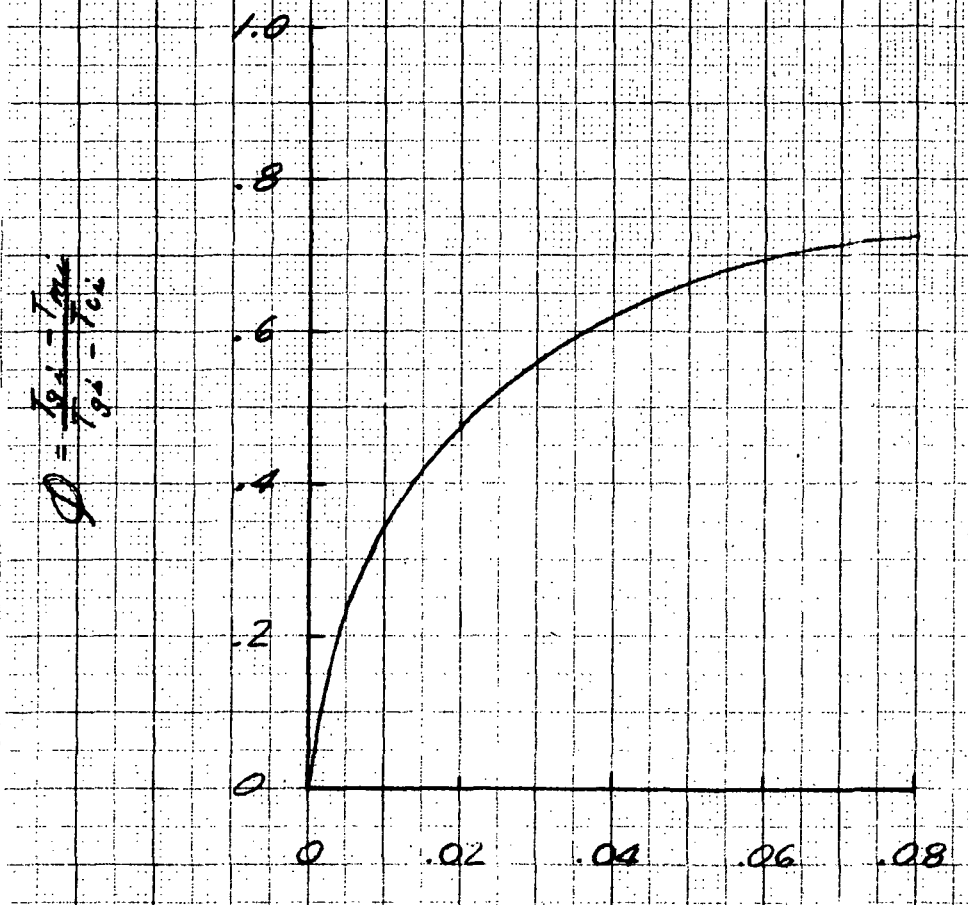

FIGURE 6 - FULL COVERAGE FILM COOLING PARAMETER

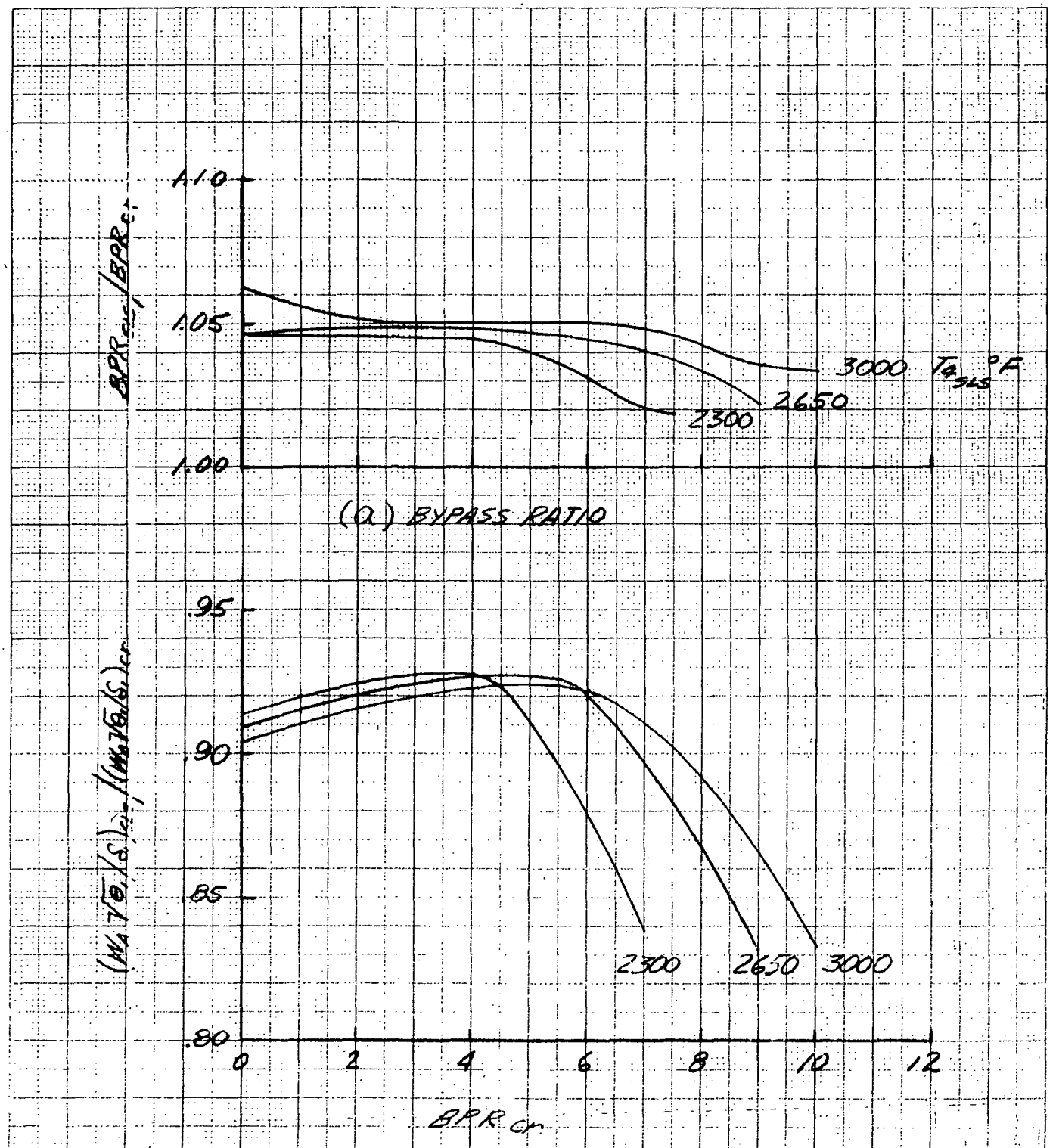

FIGURE 7. - FACTORS FOR CORRECTING CRUISE ENGINE PARAMETERS TO SEA-LEVEL-STATIC CONDITIONS. CRUISE FAN PRESSURE RATIO, 1.90; OPR_{cr}, 30.

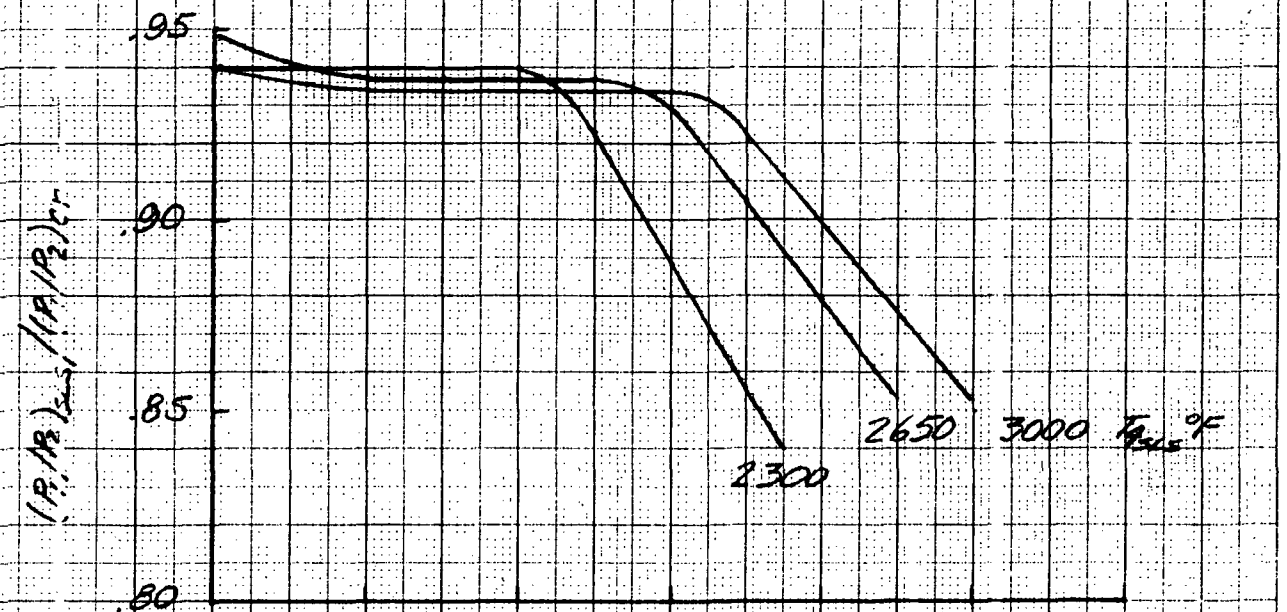

(c) FAN PRESSURE RATIO

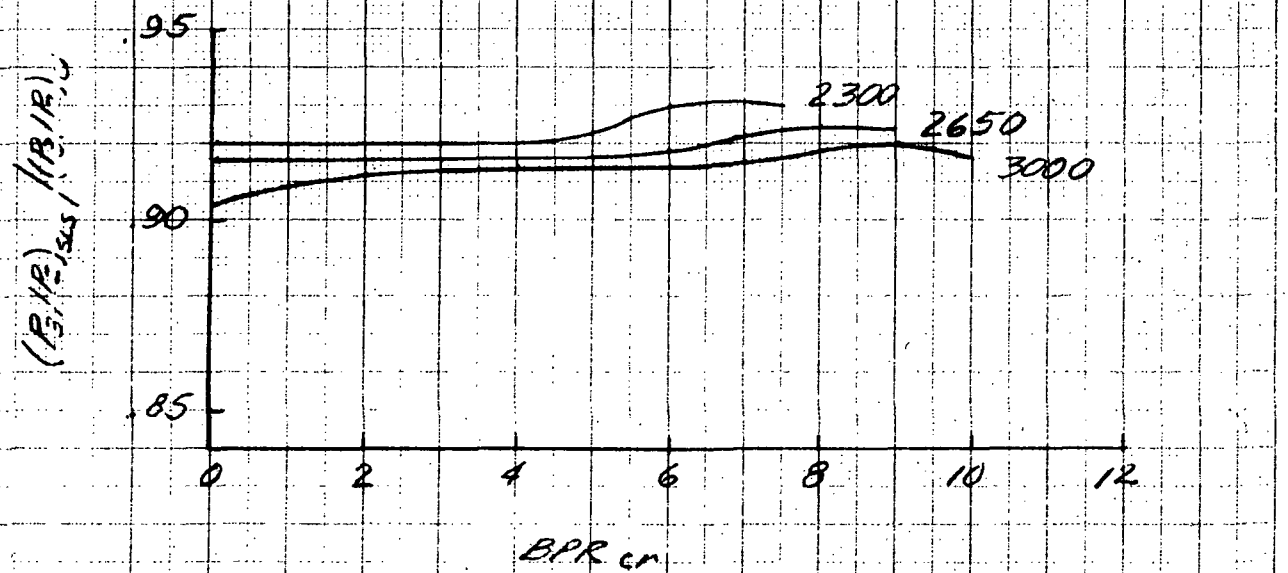

(d) INNER-COMPRESSOR PRESSURE RATIO

FIGURE 7. - CONTINUED

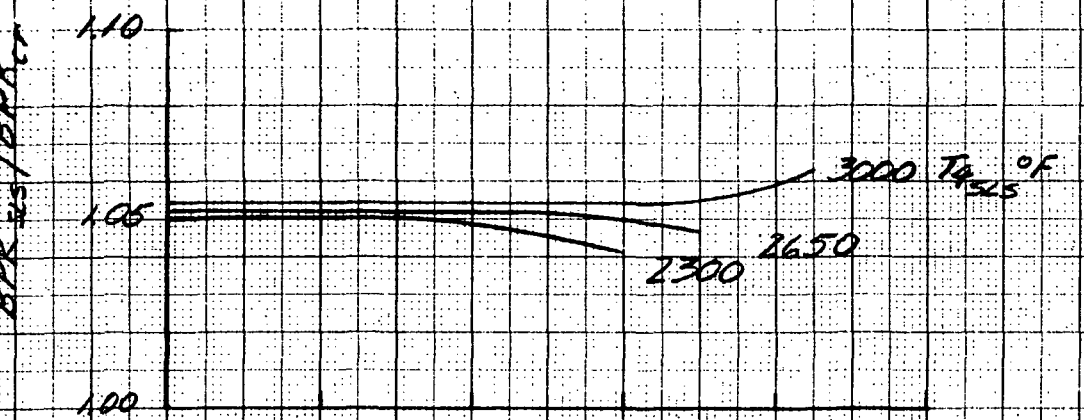

(a) BYPASS RATIO

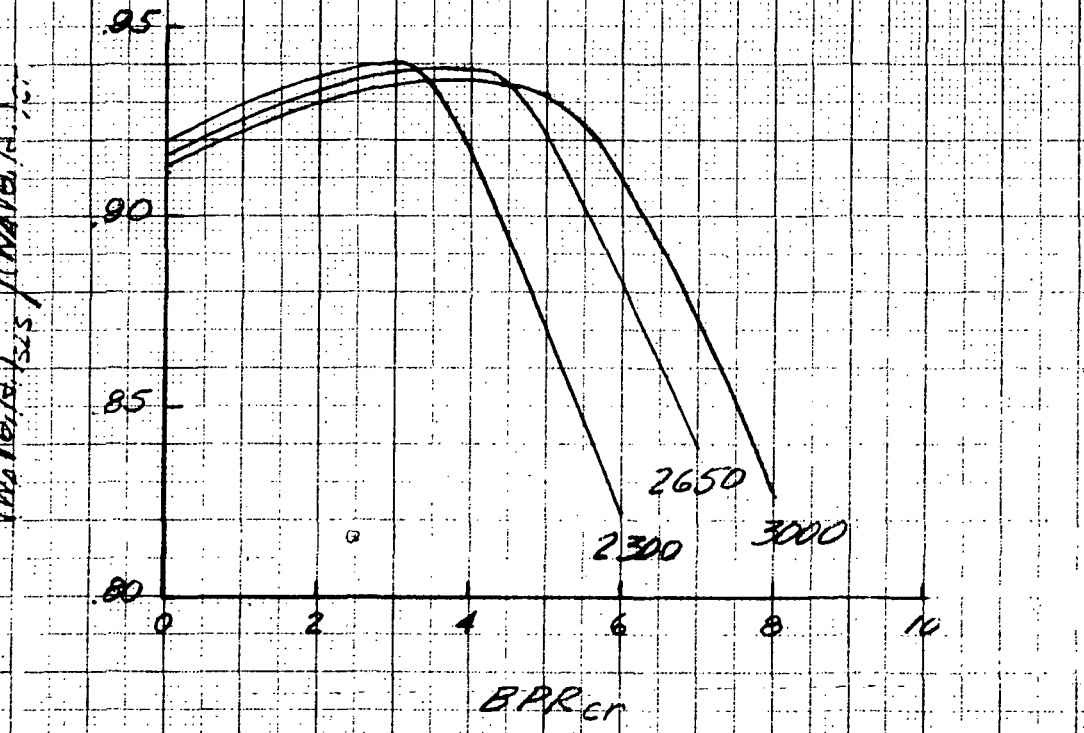

(b) TOTAL CORRECTED AIRFLOW AT FAN FACE

FIGURE 8.- FACTORS FOR CORRECTING CRUISE ENGINE PARAMETERS TO SEA-LEVEL-STATIC CONDITIONS. CRUISE FAN PRESSURE RATIO, 1.25; OPR_cr, 30.

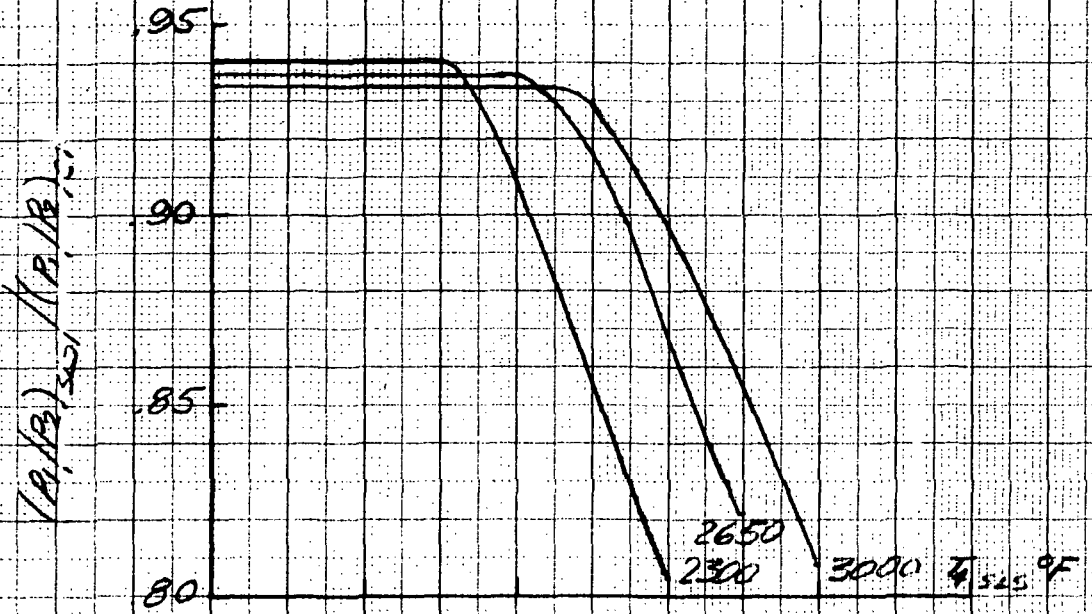

(c) FAN PRESSURE RATIO

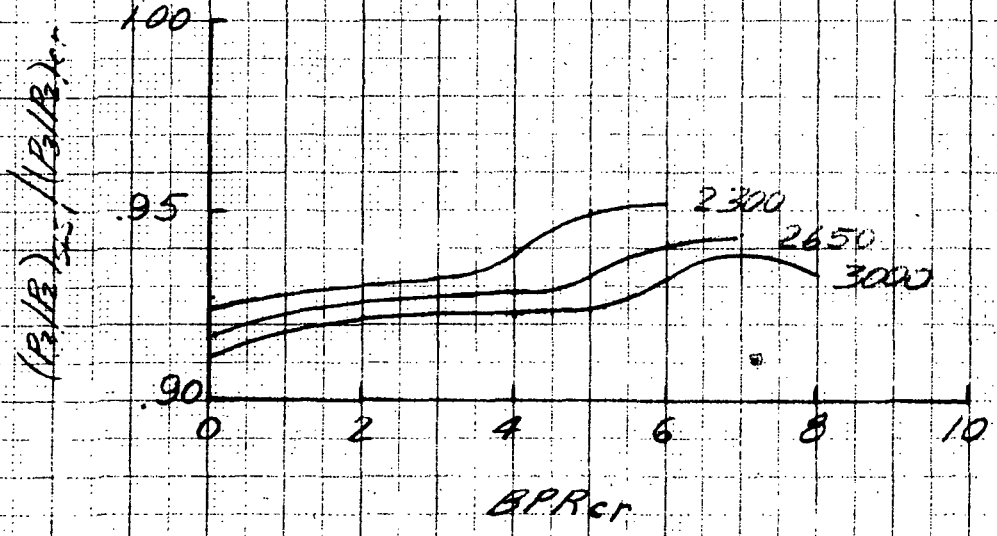

(d) INNER-COMPRESSOR PRESSURE RATIO

FIGURE 8. - CONTINUED

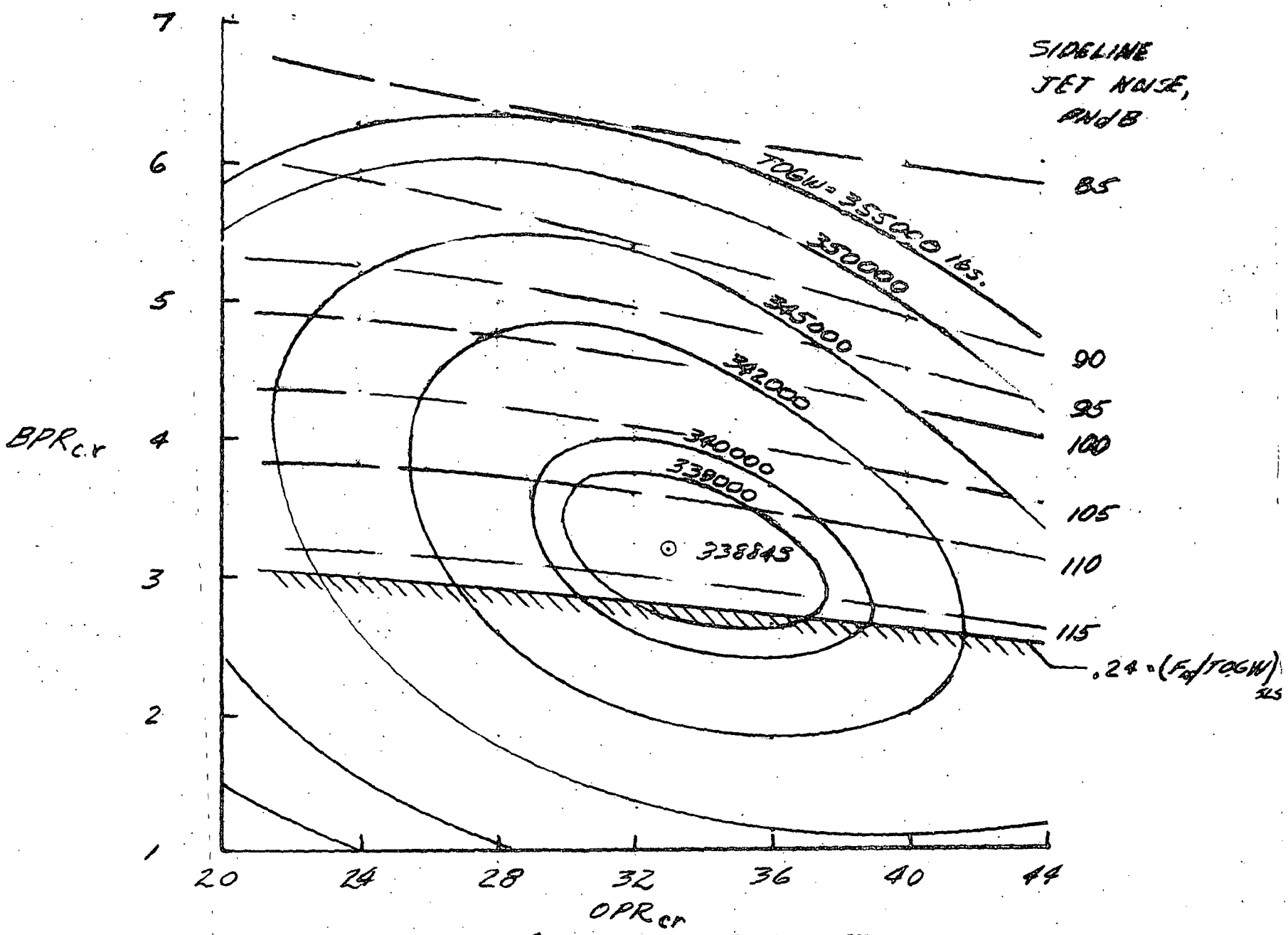

(a) CRUISE T_4, 2200°F; TAKEOFF T_4, 2300°F

FIGURE 9.- THUMBPRINT PERFORMANCE PLOTS. NO NOISE SUPPRESSION. RANGE, 3000 N. MI.; PAYLOAD, 300 PASSENGERS; FPR_{cr}, 1.90.

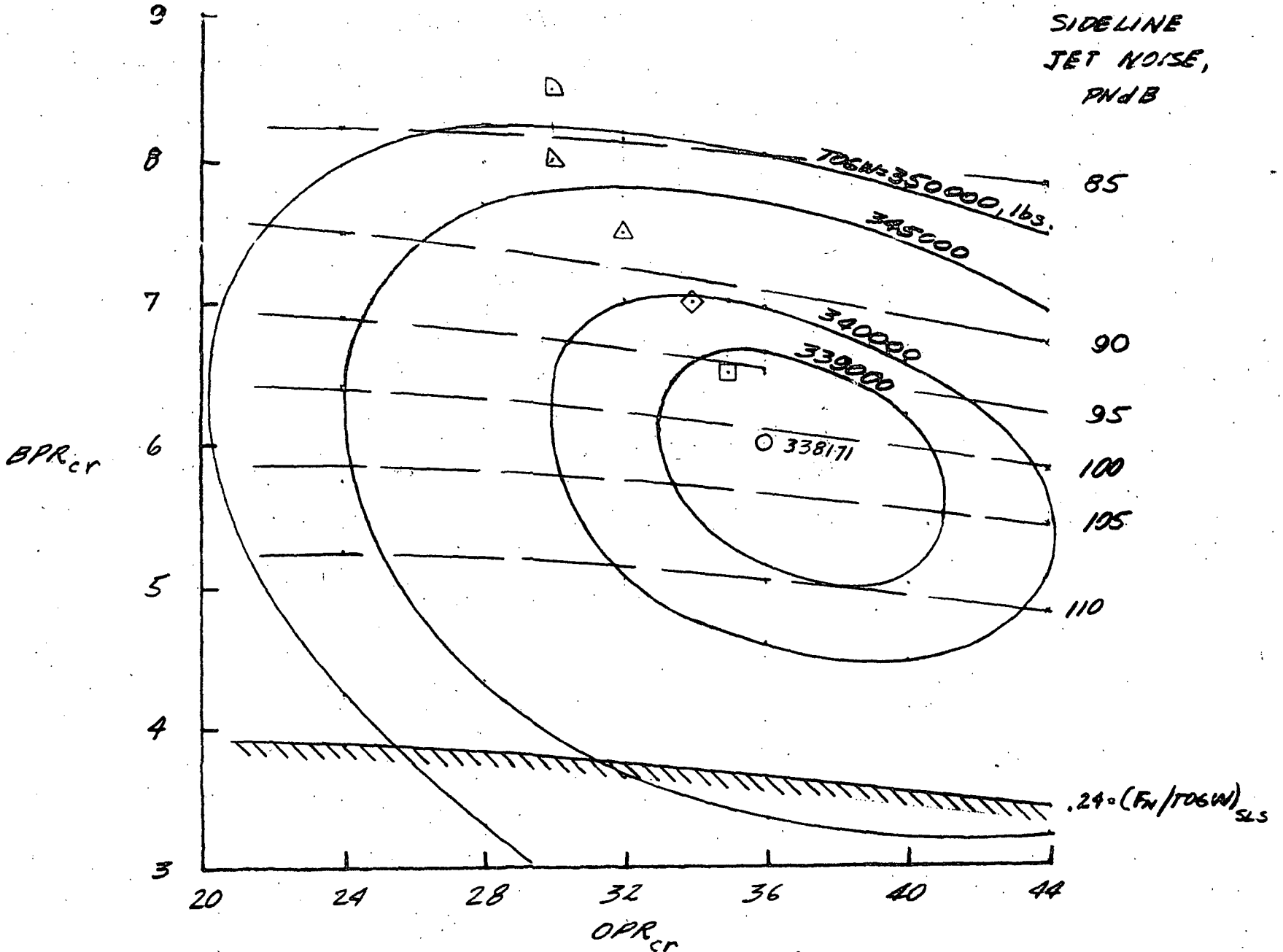

(b) CRUISE T_4, 2550°F; TAKEOFF T_4, 2650°F;

FIGURE 9. - CONTINUED

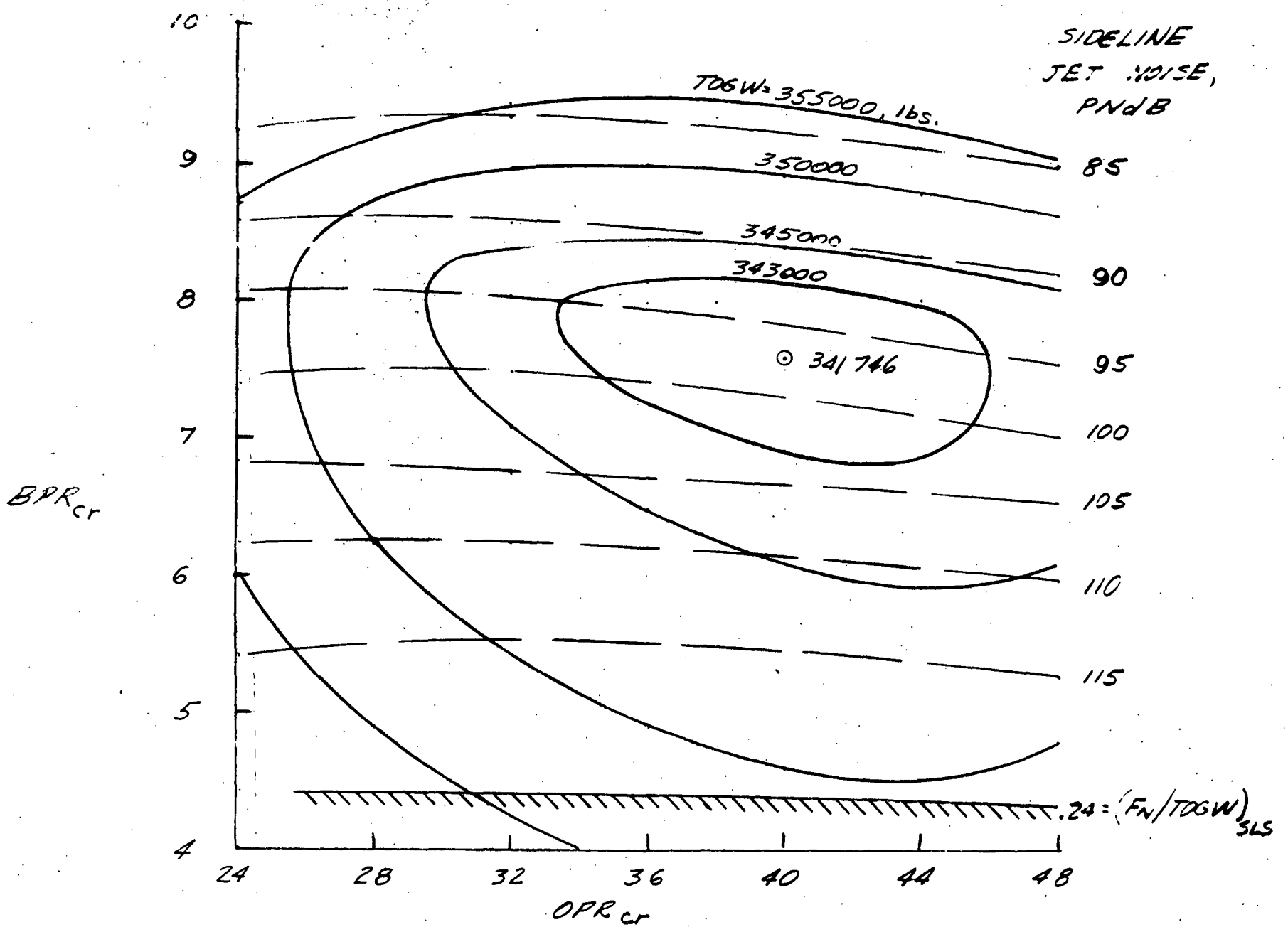

(c) CRUISE T_4, 2900°F; TAKEOFF T_4, 3000°F

FIGURE 9.- CONTINUED

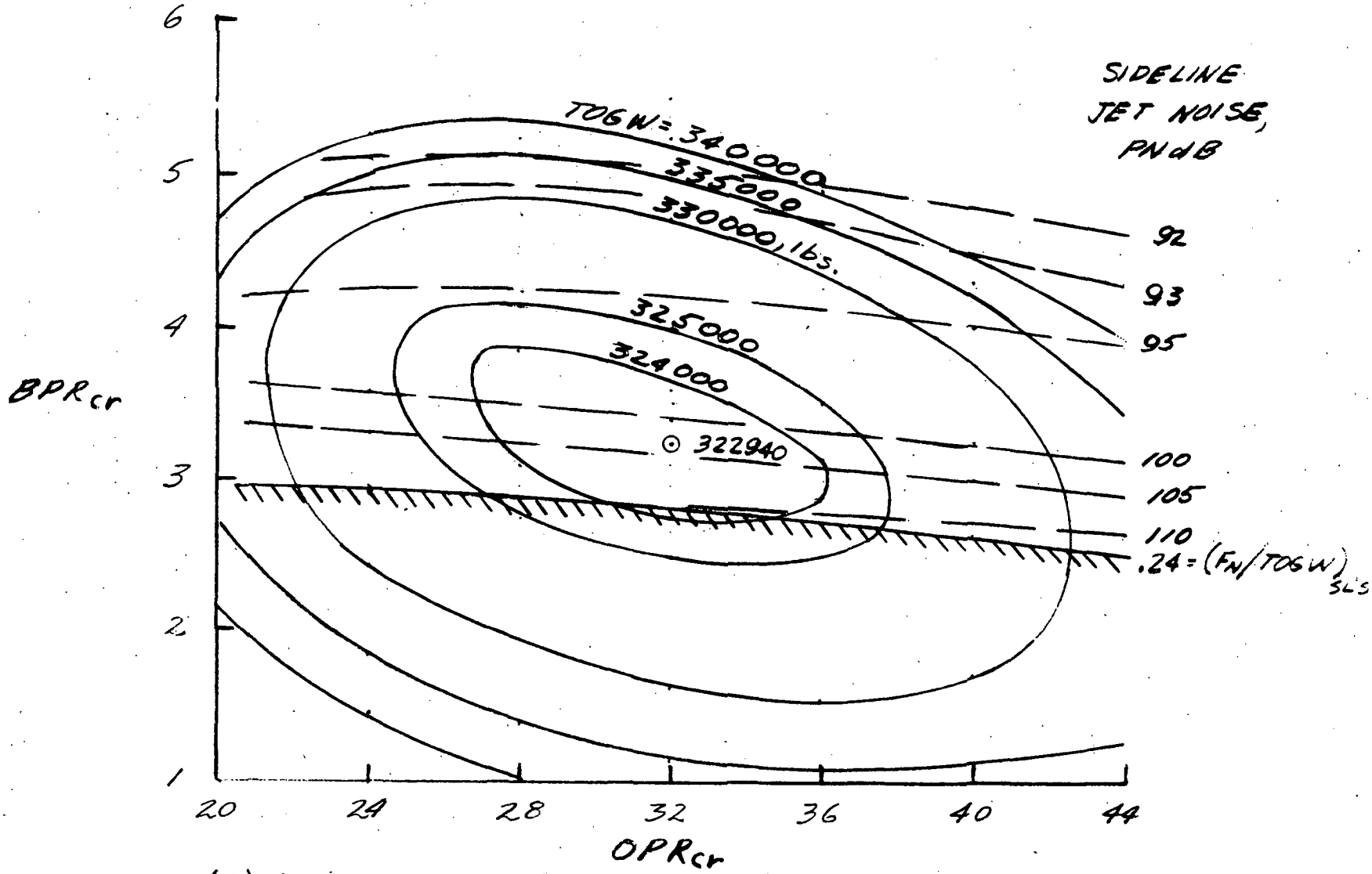

(a) CRUISE T_4, 2200°F ; TAKEOFF T_4, 2300°F.

FIGURE 10. - THUMBPRINT PERFORMANCE PLOTS. NO NOISE SUPPRESSION. RANGE, 3000 N. MI.; PAYLOAD, 300 PASSENGERS; $FPR_{cr} = 2.25$.

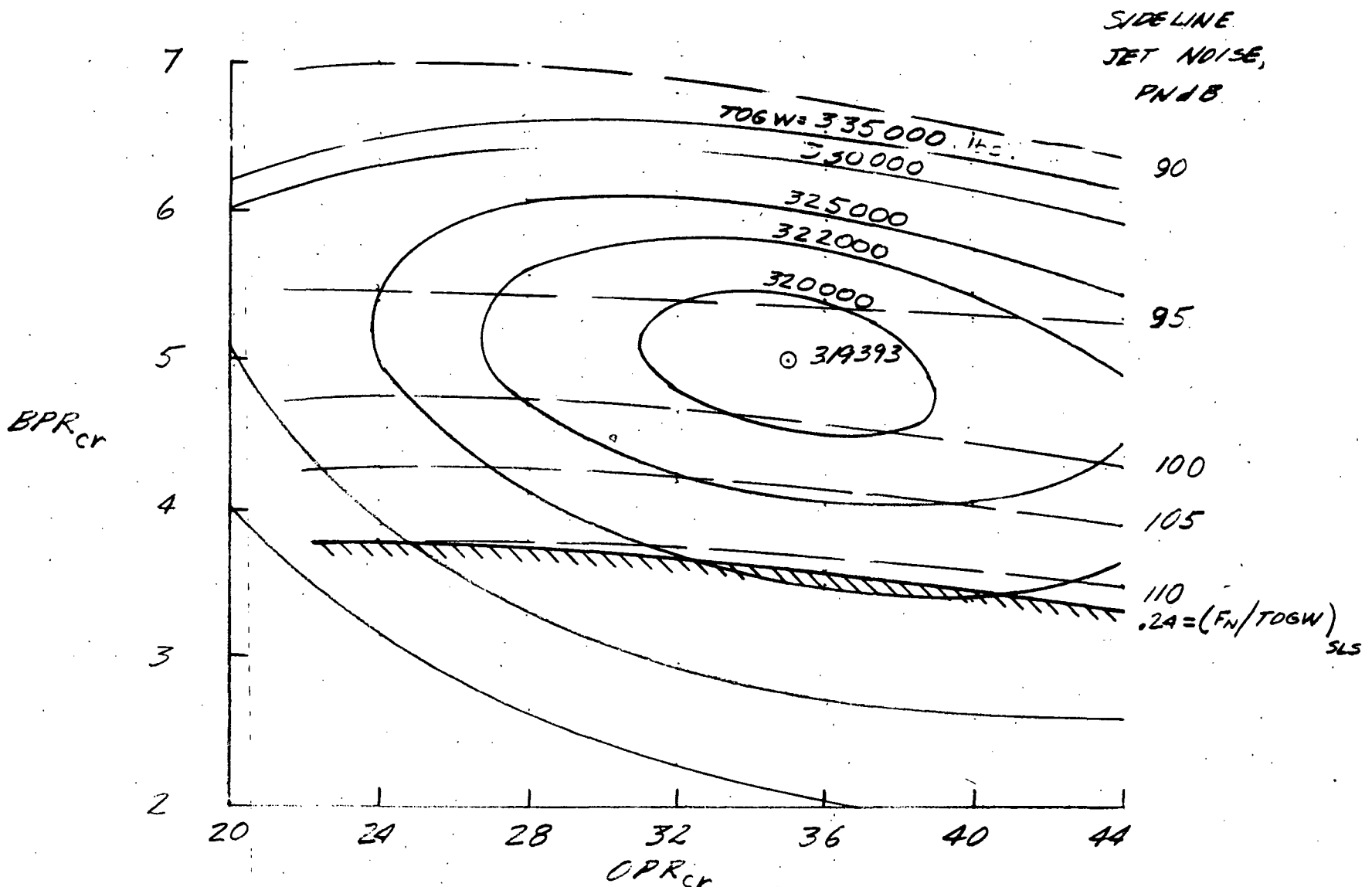

(b) CRUISE T_4, 2550°F; TAKEOFF T_4, 2650°F.

FIGURE 10.- CONTINUED

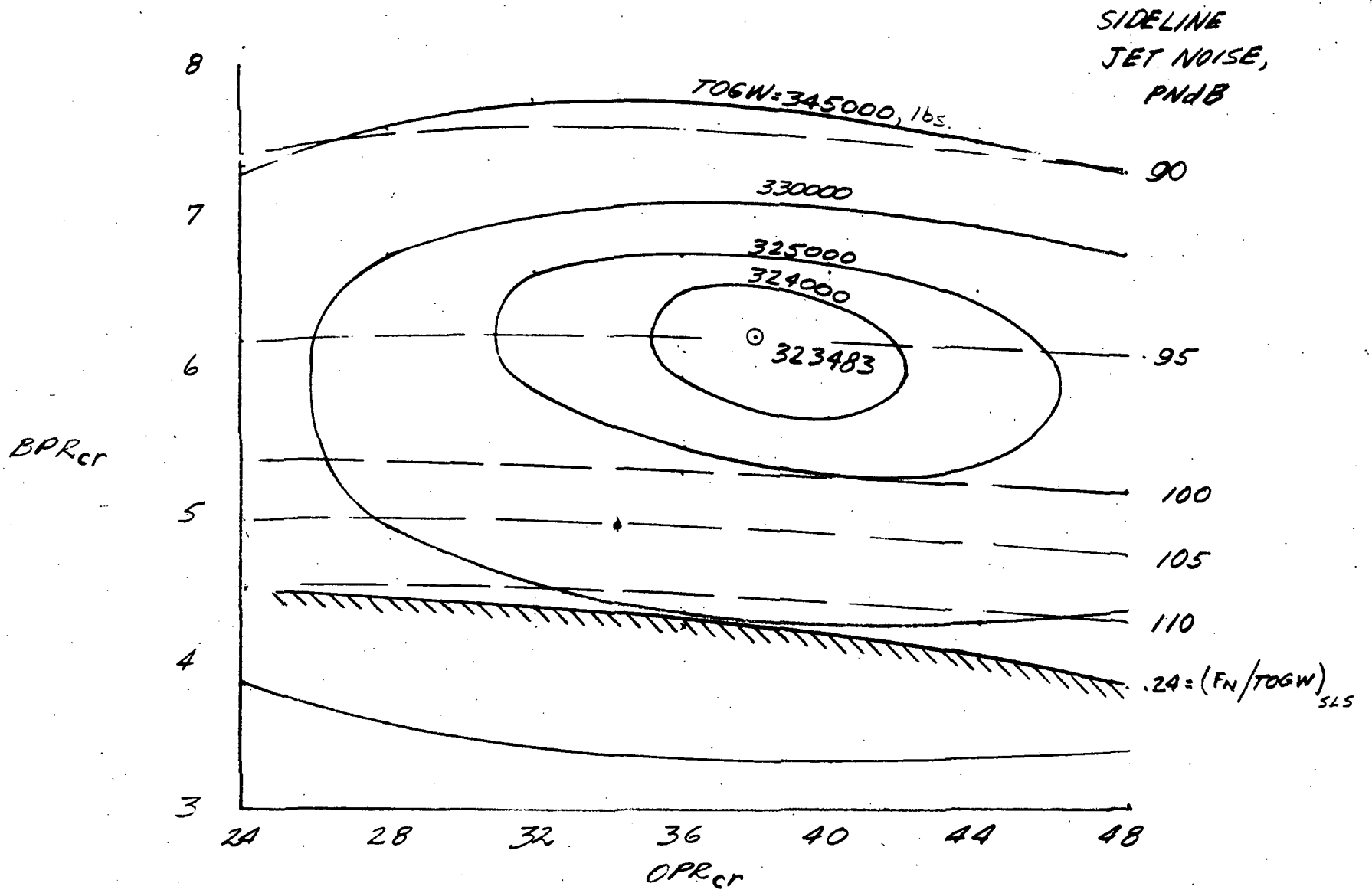

(c) CRUISE T_4, 2900°F; TAKEOFF T_4 = 3000°F.

FIGURE 10. - CONTINUED

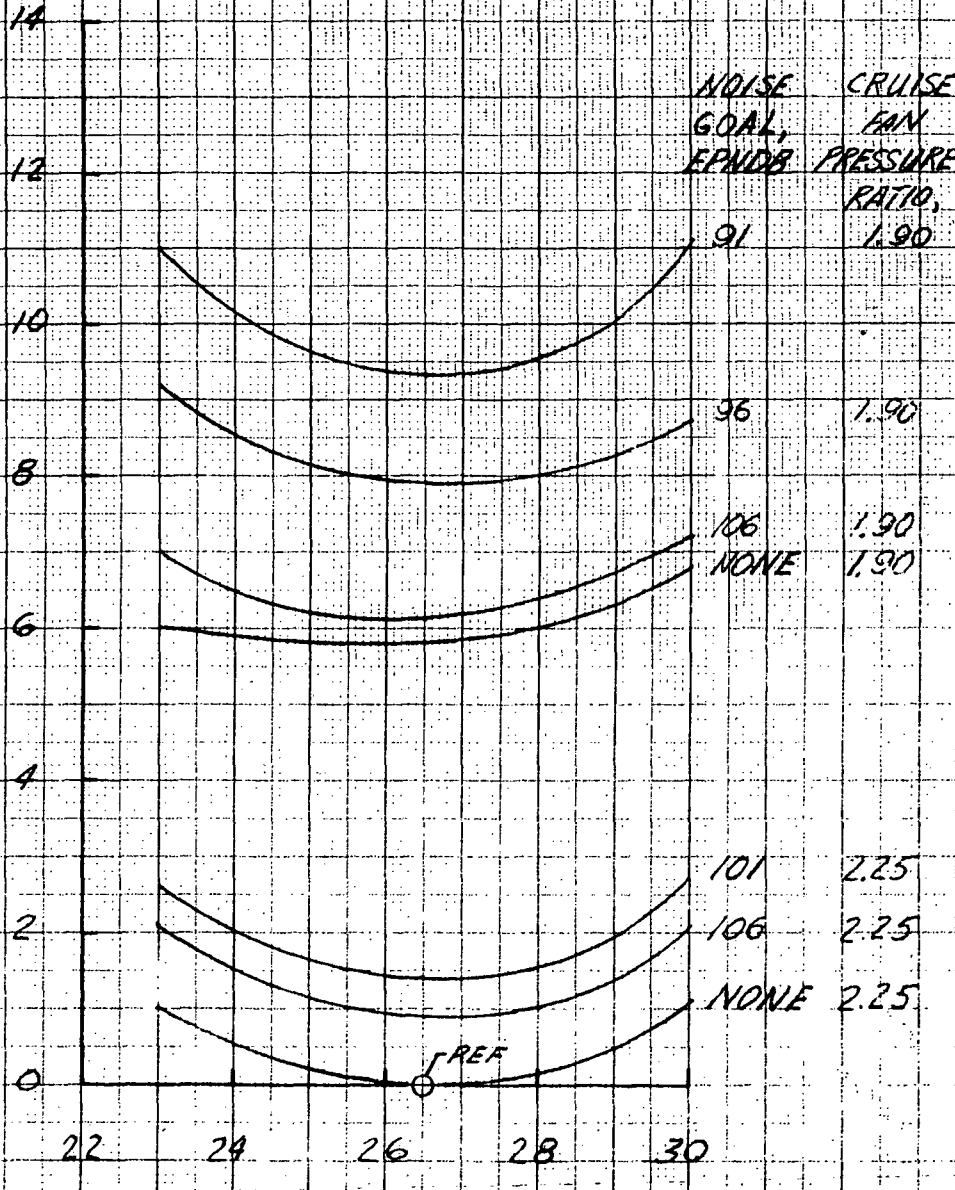

FIGURE 11. - EFFECT OF TURBINE-INLET-TEMPERATURE ON THE OPTIMUM TOGW AT NOISE GOALS OF 106, 101, 96, AND 91 EPNdB. EPR_{cr} = 1.90 (SINGLE-STAGE) AND 2.25 (TWO-STAGE); RANGE, 3000 N.MI.; PAYLOAD, 300 PASSENGERS.

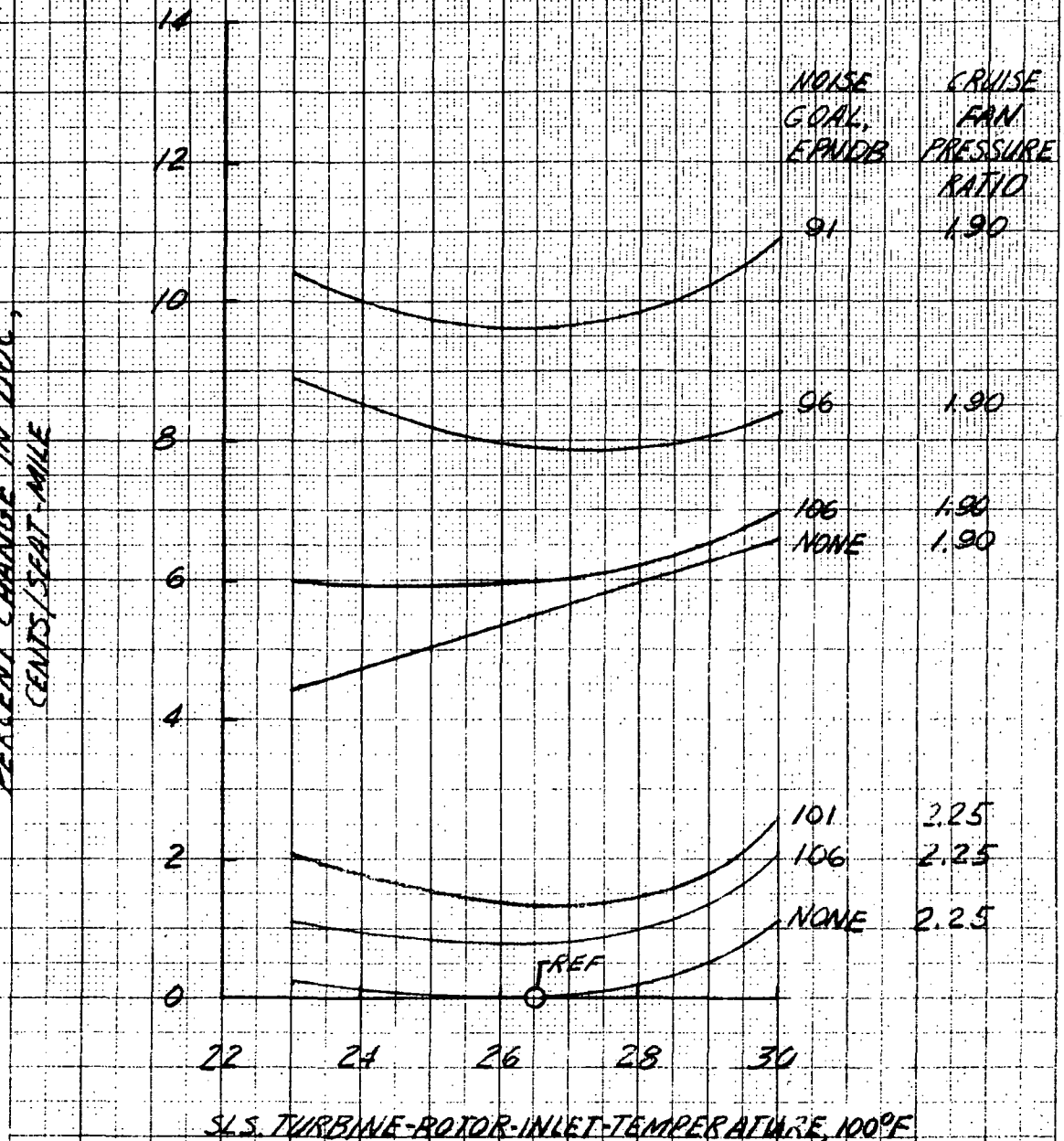

FIGURE 12.- EFFECT OF TURBINE-INLET-TEMPERATURE ON DOC AT NOISE GOALS OF 106, 101, 96, AND 91 EPNdB. FPR_{cr}, 1.90 (SINGLE-STAGE) AND 2.25 (TWO-STAGE); RANGE, 3000 N. MI.; PAYLOAD, 300 PASSENGERS.

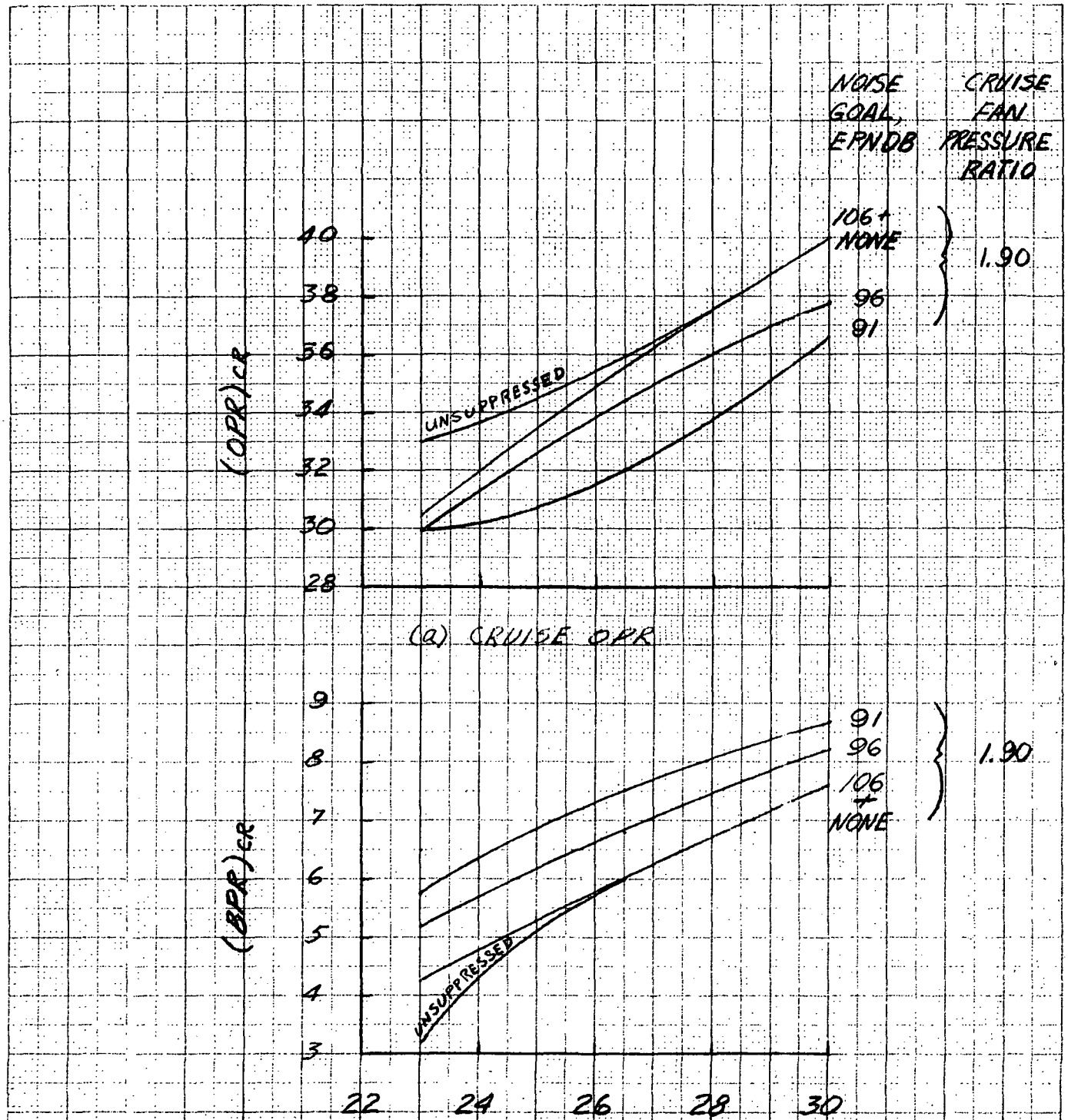

FIGURE 13.- EFFECT OF TURBINE-INLET-TEMPERATURE ON THE ENGINE DESIGN CHARACTERISTICS OF TOGW-OPTIMIZED CYCLES. FPR of 1.90 (SINGLE-STAGE) AND 2.25 (TWO-STAGE), RANGE, 3000 N.MI.; PAYLOAD, 300 PASSENGERS.

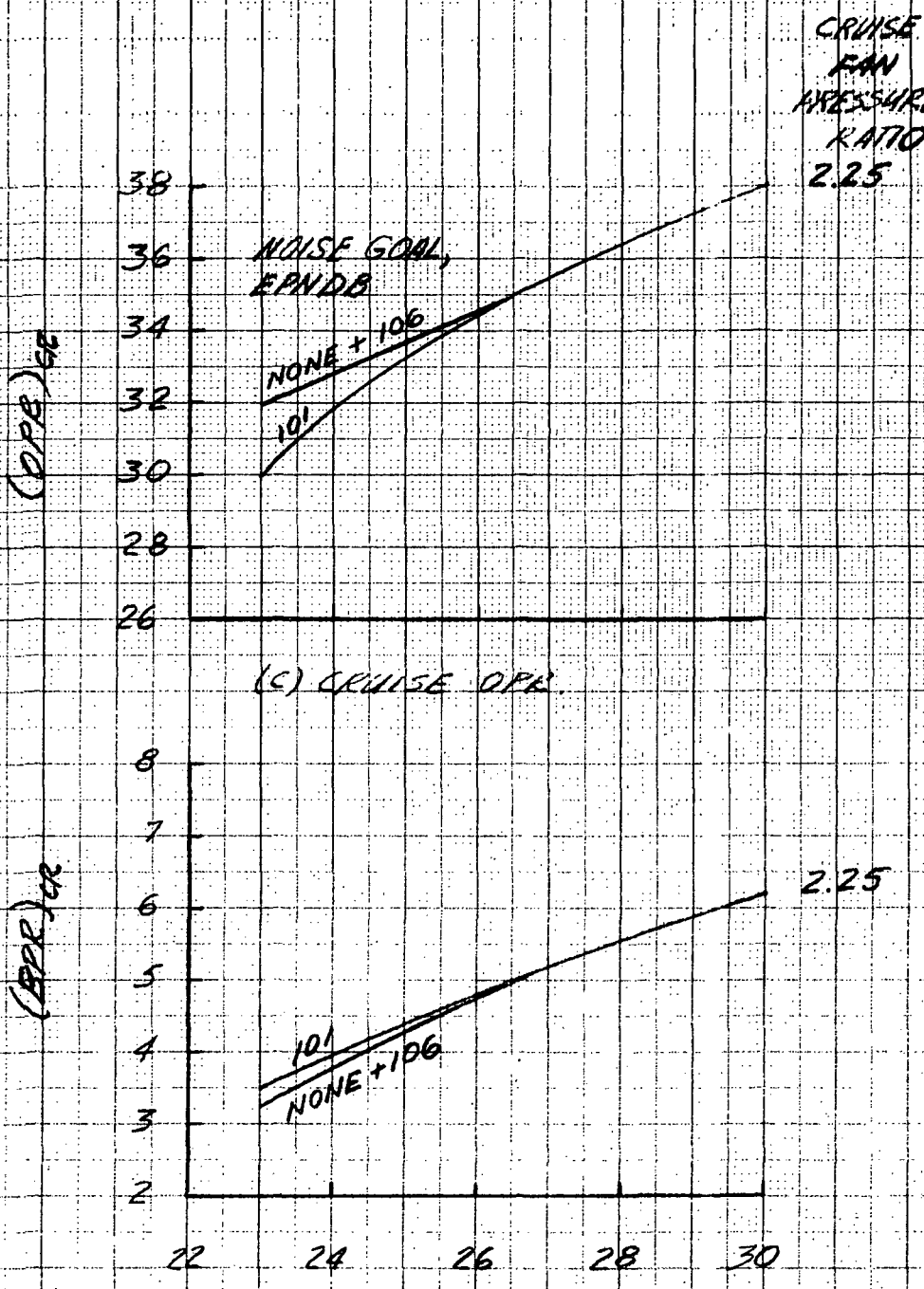

(c) CRUISE OPR

S.L.S. TURBINE-ROTOR-INLET-TEMPERATURE, 100°F

(d) CRUISE BPR

FIGURE 13. - CONTINUED

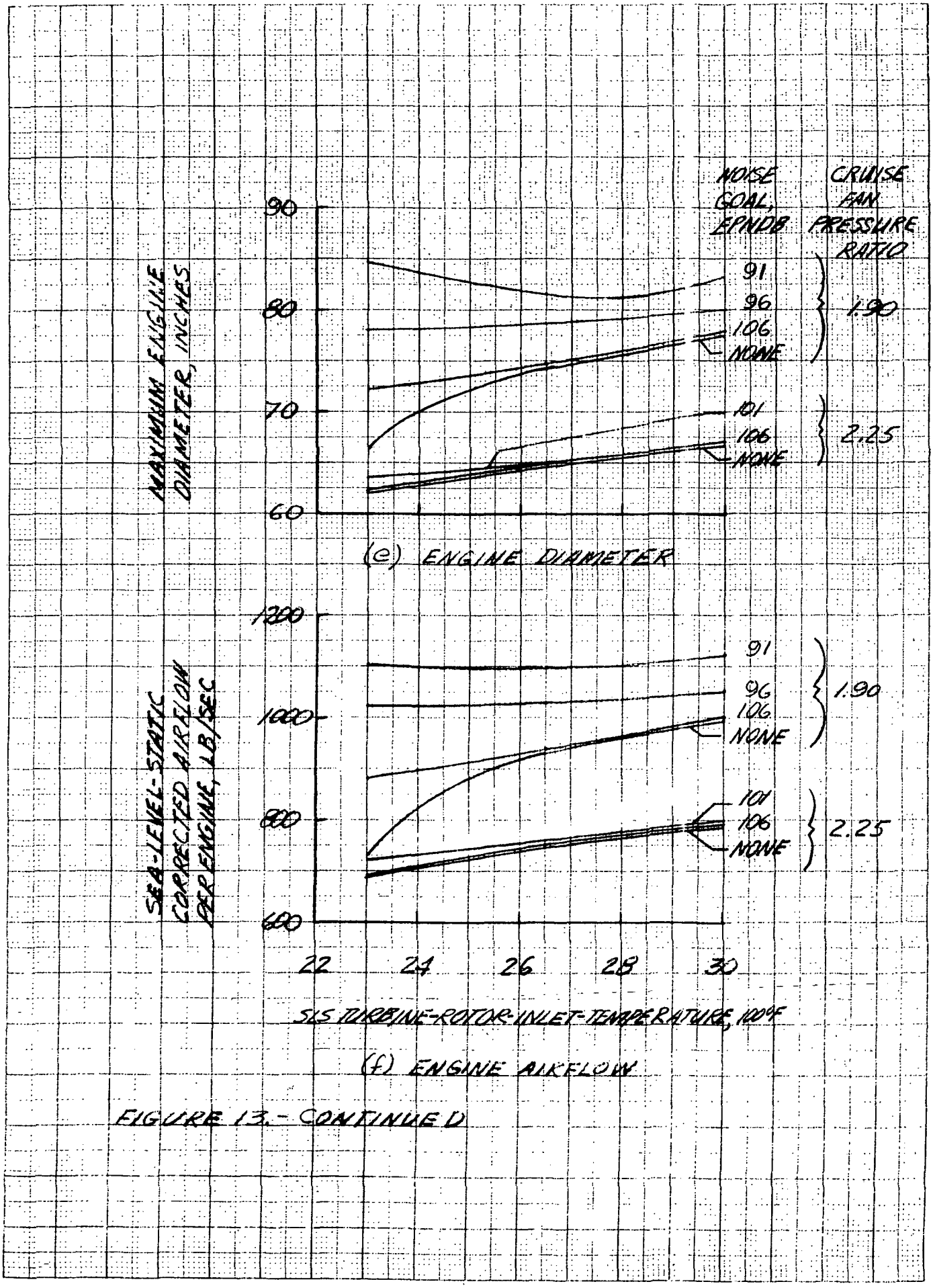

FIGURE 13.- CONTINUED

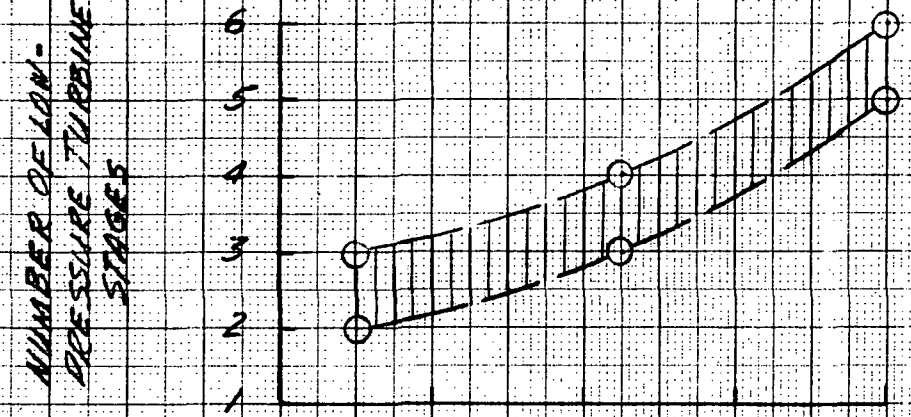

(g) NUMBER OF TURBINE STAGES

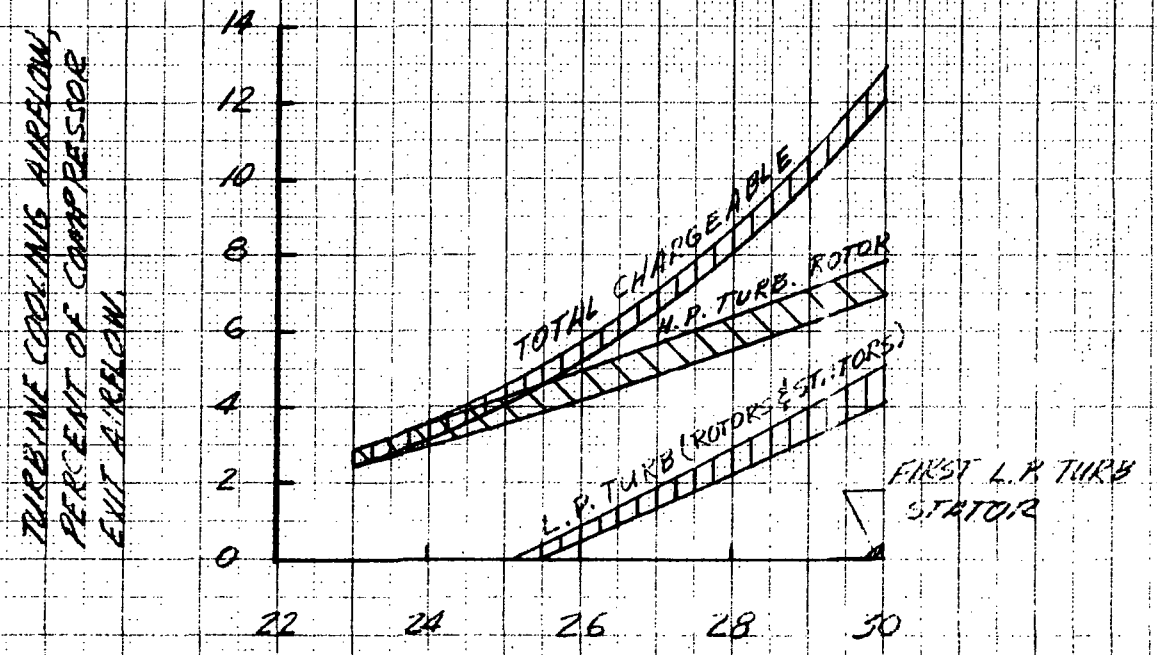

SLS TURBINE-ROTOR-INLET-TEMPERATURE, 100°F

(h) TURBINE COOLING BLEED

FIGURE 13 - CONTINUED

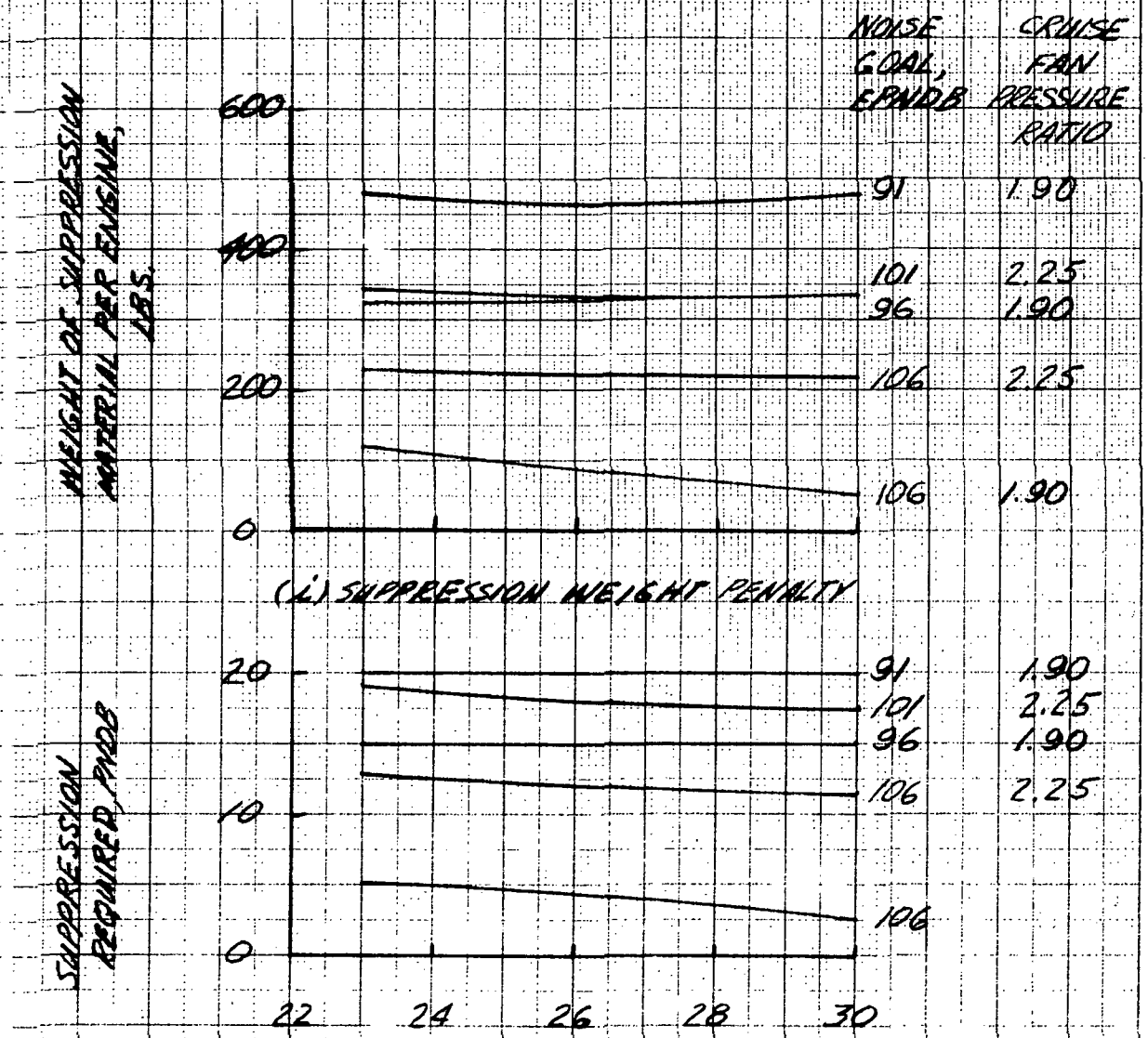

FIGURE 13.- CONTINUED

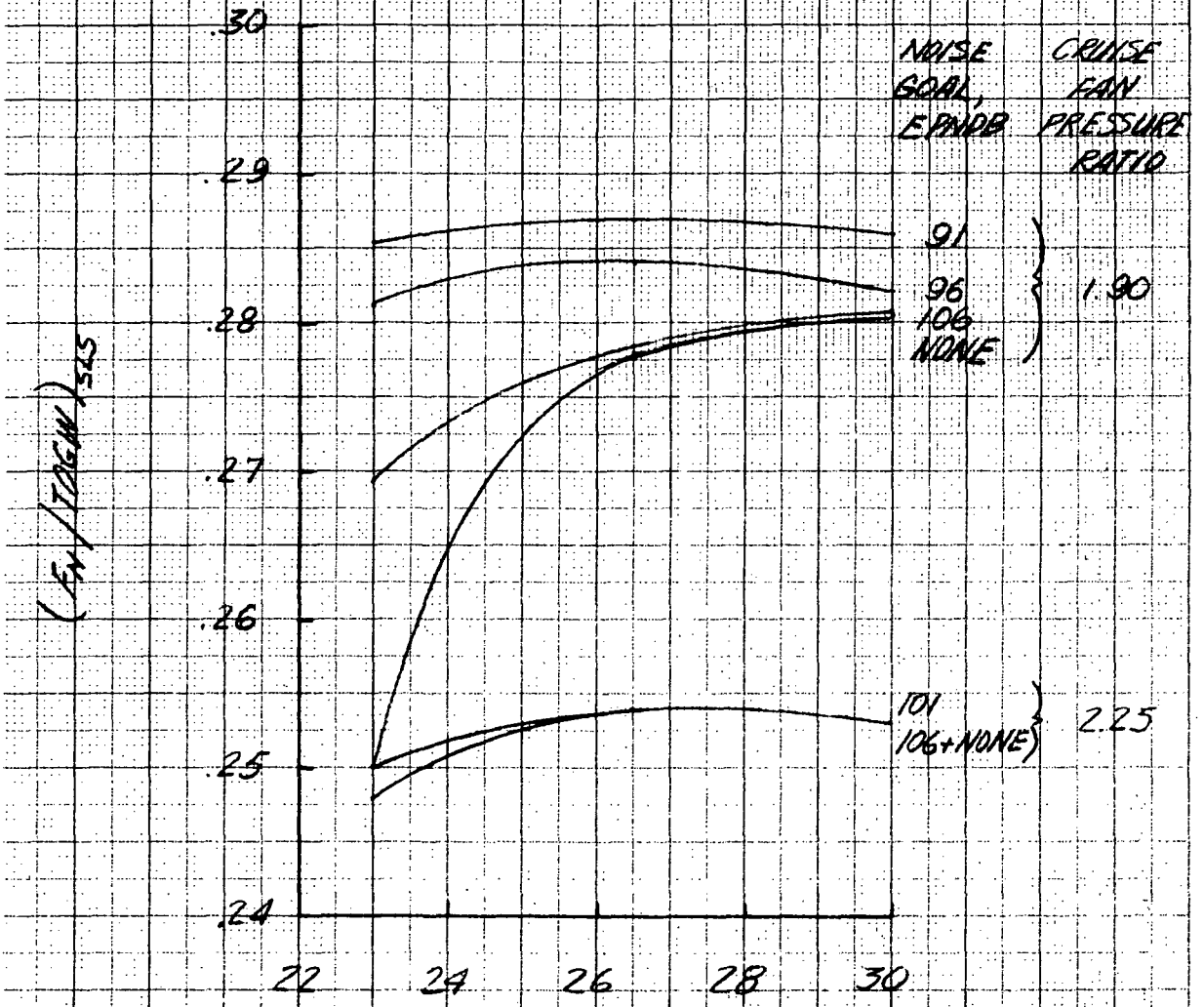

(k). THRUST TO GROSS WEIGHT RATIO

FIGURE 13. - CONTINUED

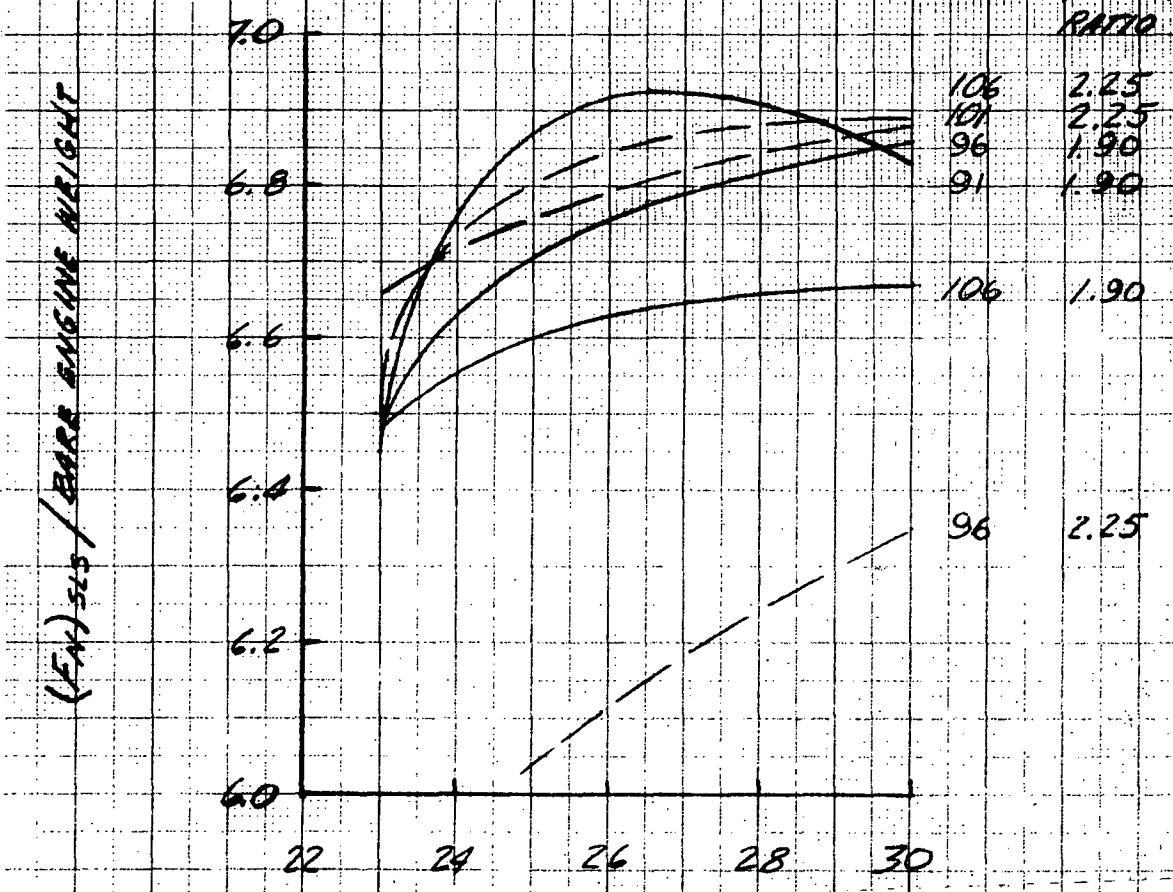

(1) BARE ENGINE, THRUST TO WEIGHT, SLS.

FIGURE 13. - CONTINUED

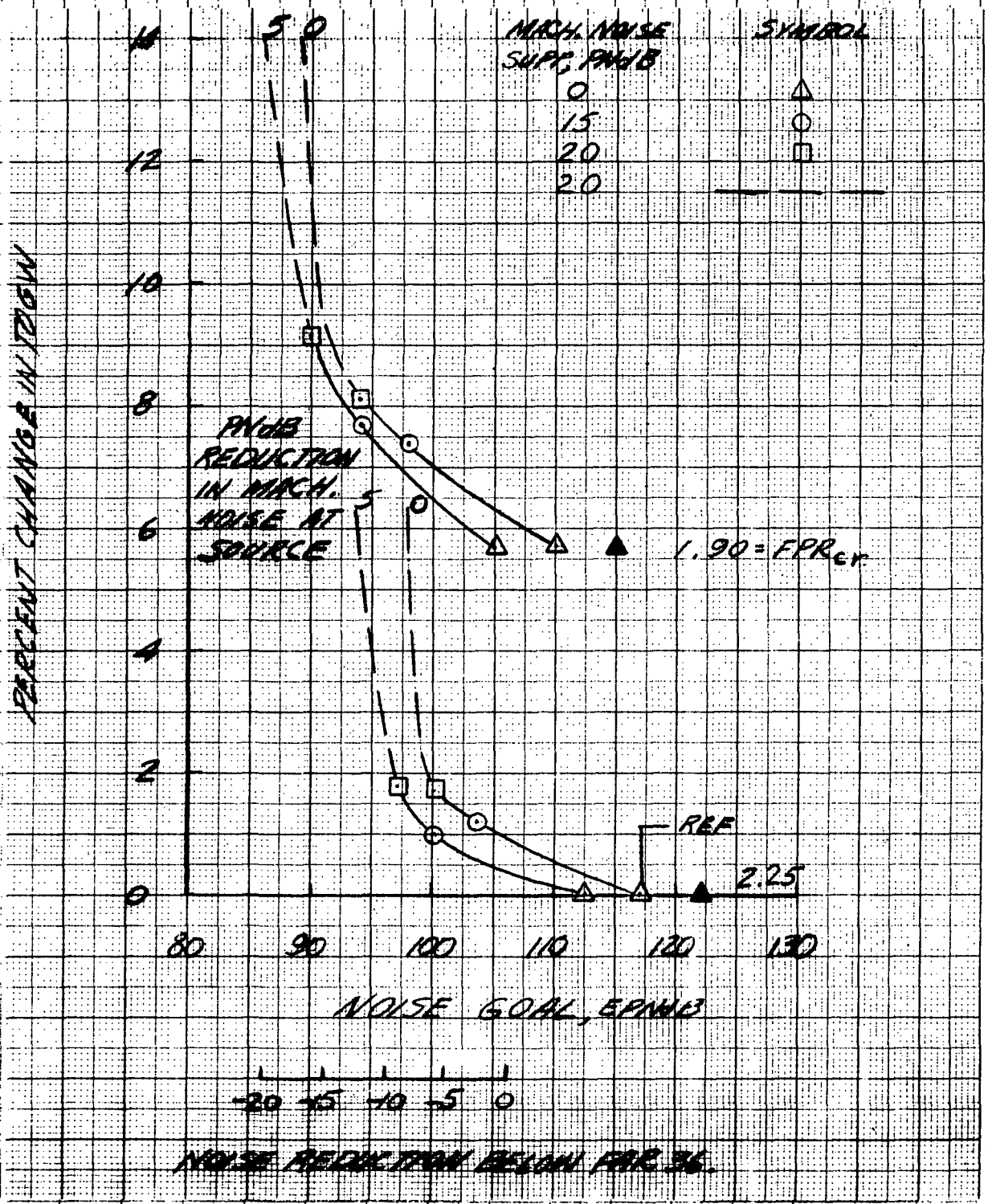

FIGURE 14 - TOGW PENALTY VERSUS NOISE GOAL. $T_{4_{SLS}} = 2650°F$; $T_{4_{CR}} = 2550°F$; $FPR_{cr} = 1.9$ (1-STAGE) AND 2.25 (2-STAGE); $M_{CR} = 0.98$; CRUISE ALTITUDE = 42000 FT.; RANGE = 3000 N. MI.; PAYLOAD = 300 PASSENGERS.

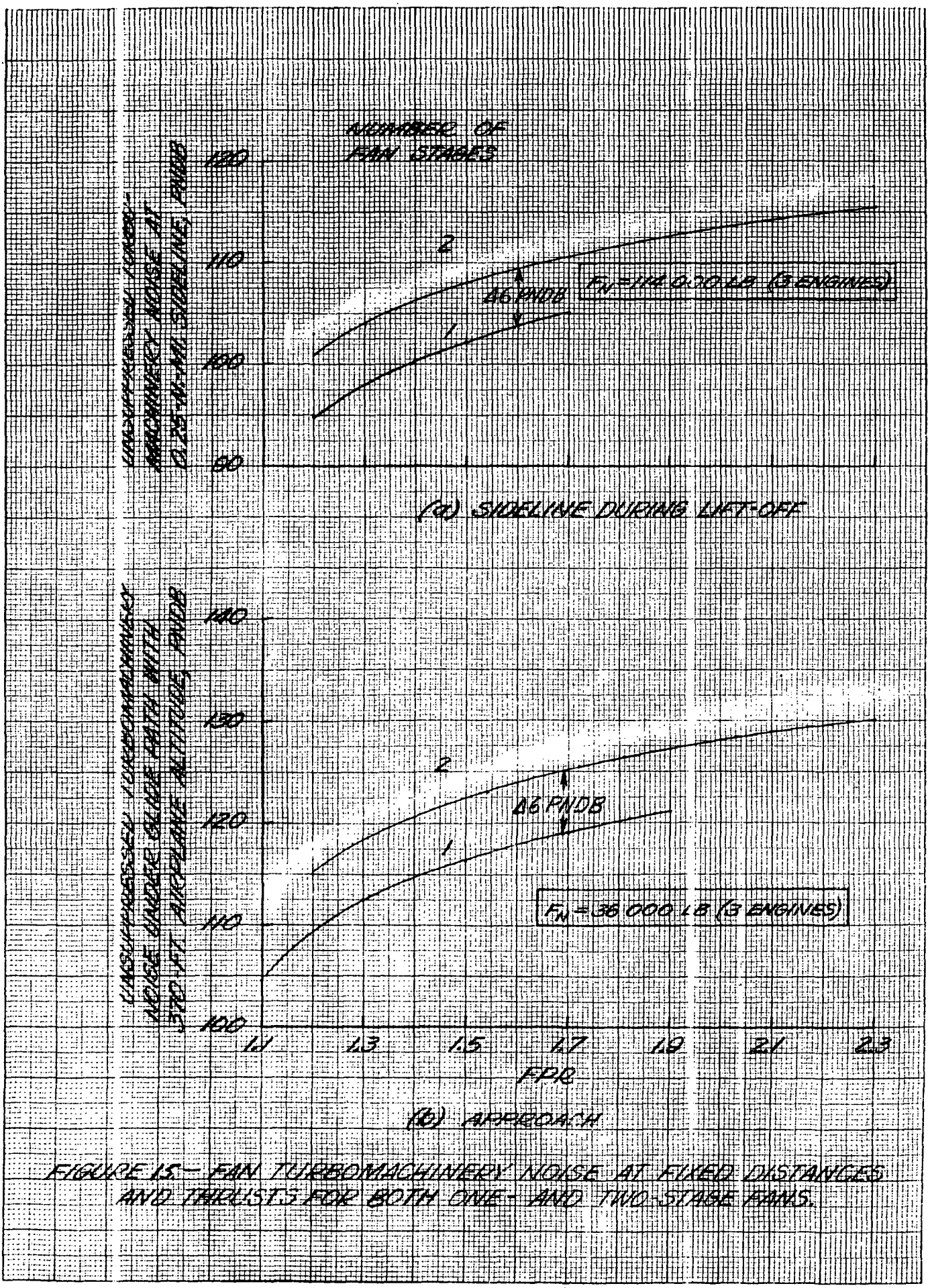

FIGURE 15 — FAN TURBOMACHINERY NOISE AT FIXED DISTANCES AND THRUSTS FOR BOTH ONE- AND TWO-STAGE FANS.

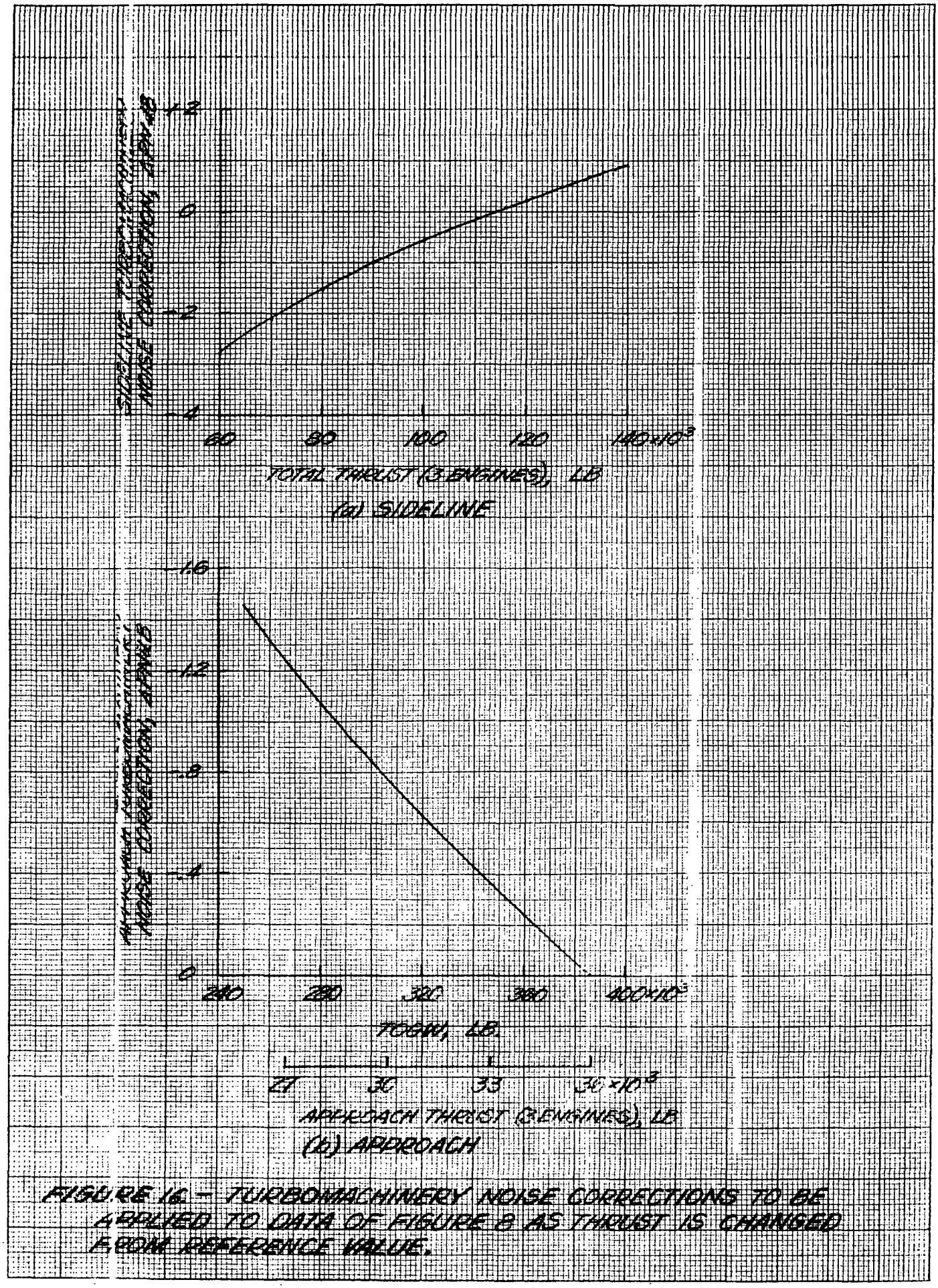

FIGURE 16 – TURBOMACHINERY NOISE CORRECTIONS TO BE APPLIED TO DATA OF FIGURE 8 AS THRUST IS CHANGED FROM REFERENCE VALUE.

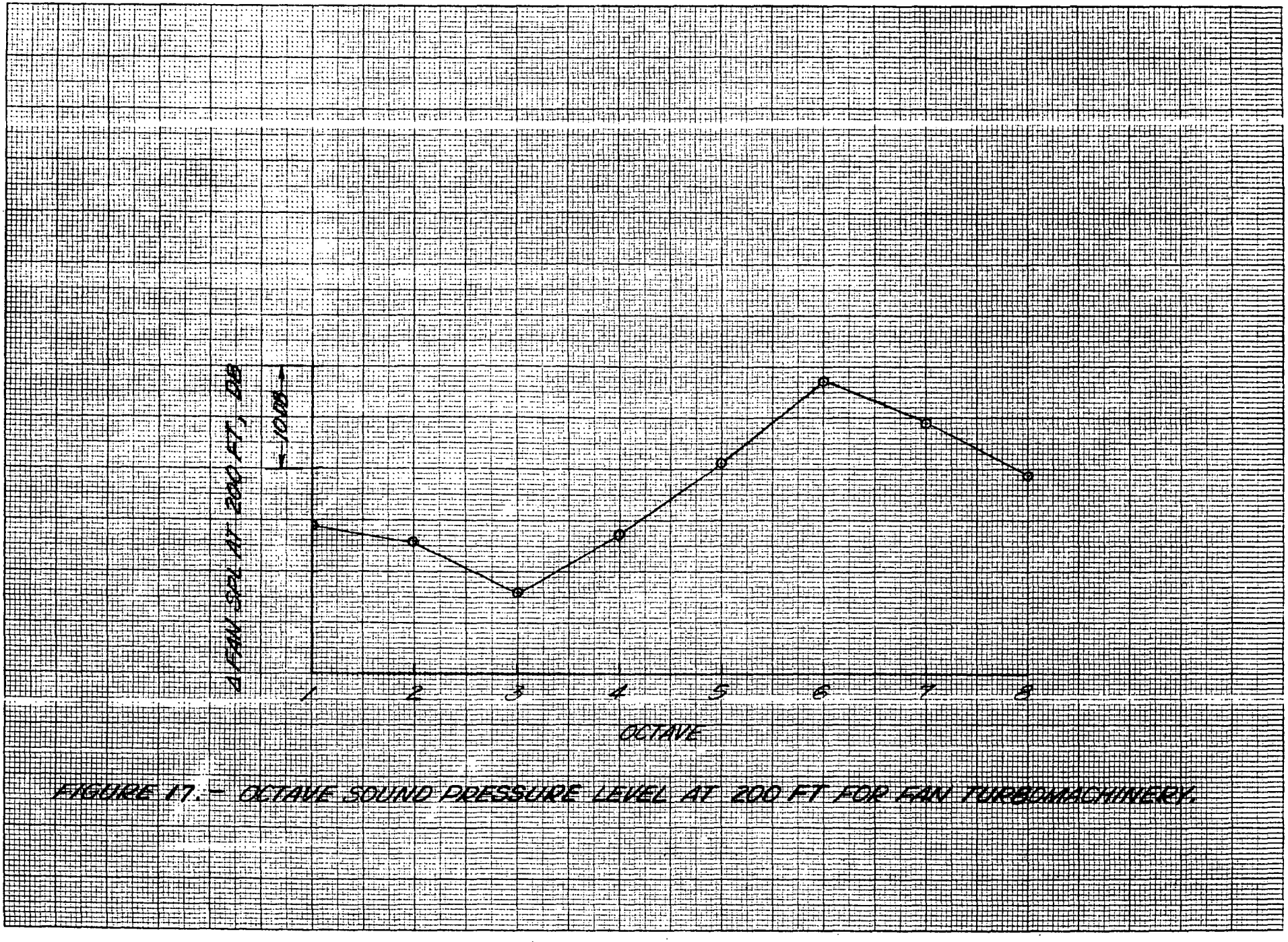

FIGURE 17. – OCTAVE SOUND PRESSURE LEVEL AT 200 FT FOR FAN TURBOMACHINERY.

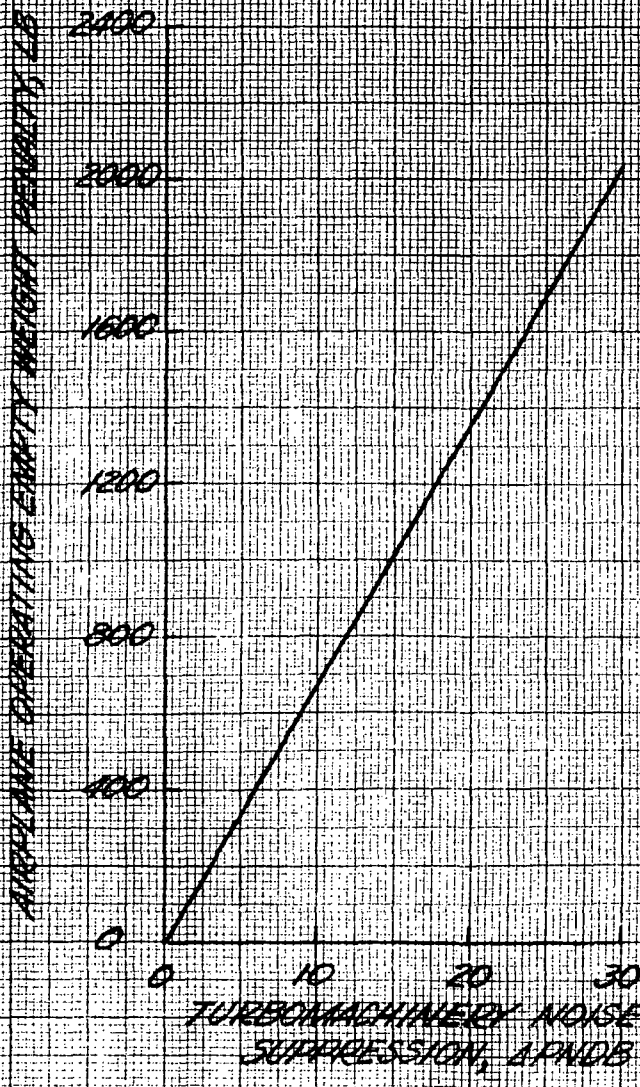

FIGURE 18 – AIRPLANE OPERATING-EMPTY-WEIGHT PENALTY RELATED TO FAN TURBOMACHINERY NOISE SUPPRESSION FOR A THREE-ENGINE AIRPLANE WITH NOMINAL 80-IN. DIAMETER ENGINES.

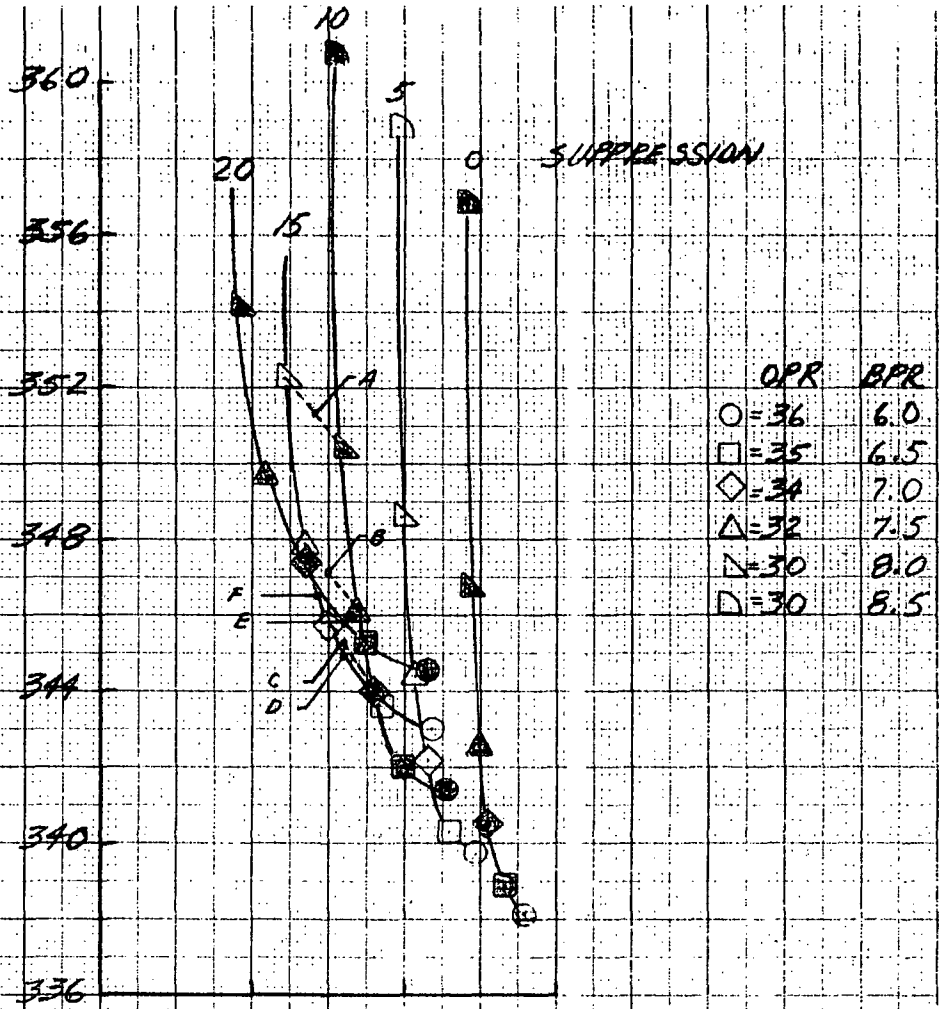

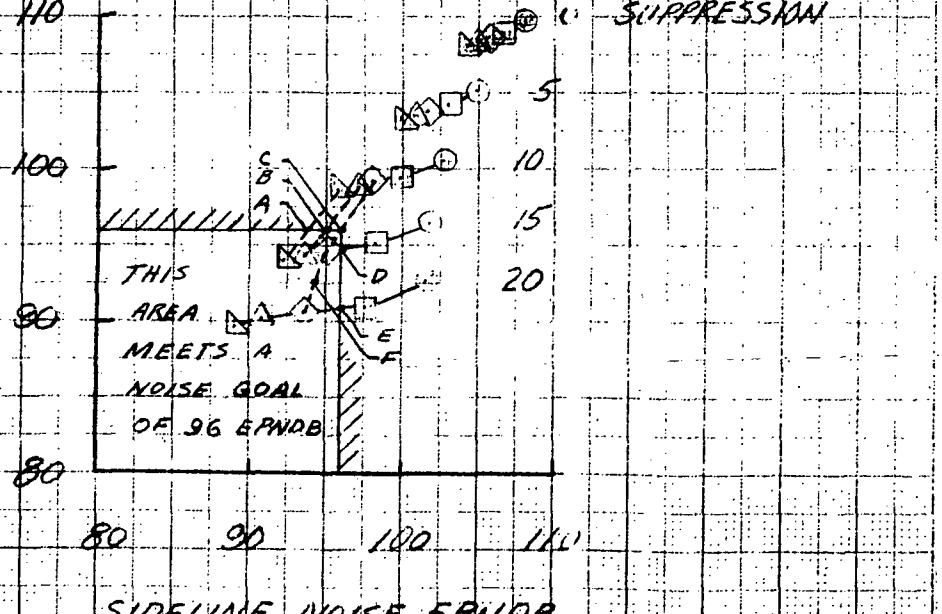

FIGURE 19. - OPTIMIZATION WORKING PLOT. TOGW AND APPROACH NOISE VERSUS SIDELINE NOISE. EPR_{cr}, 1.90, FAN NOISE SUPPRESSION, 0 TO 20 PNDB